SCIENTIFIC REPORTS

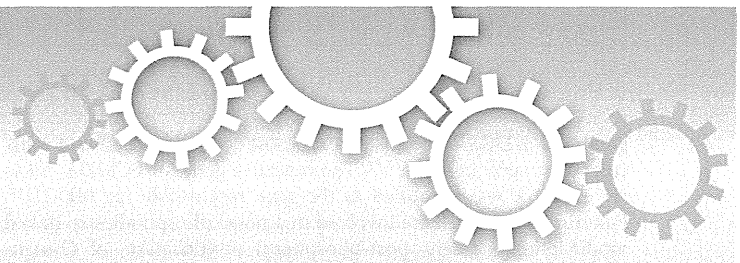

OPEN

SUBJECT AREAS:
DISEASES
GENETICS

Received
8 October 2014

Accepted
13 January 2015

Published
9 February 2015

Correspondence and requests for materials should be addressed to T.T. (toda@med.kobe-u.ac.jp)

Fukutin is prerequisite to ameliorate muscular dystrophic phenotype by myofiber-selective LARGE expression

Yoshihisa Ohtsuka[1], Motoi Kanagawa[1], Chih-Chieh Yu[1], Chiyomi Ito[1], Tomoko Chiyo[2], Kazuhiro Kobayashi[1], Takashi Okada[2], Shin'ichi Takeda[2] & Tatsushi Toda[1]

[1]Division of Neurology/Molecular Brain Science, Kobe University Graduate School of Medicine, Kobe, 650-0017, Japan, [2]Department of Molecular Therapy, National Institute of Neuroscience, National Center of Neurology and Psychiatry, Kodaira, 187-8502, Japan.

α-Dystroglycanopathy (α-DGP) is a group of muscular dystrophy characterized by abnormal glycosylation of α-dystroglycan (α-DG), including Fukuyama congenital muscular dystrophy (FCMD), muscle-eye-brain disease, Walker-Warburg syndrome, and congenital muscular dystrophy type 1D (MDC1D), etc. LARGE, the causative gene for MDC1D, encodes a glycosyltransferase to form [-3Xyl-α1,3GlcAβ1-] polymer in the terminal end of the post-phosphoryl moiety, which is essential for α-DG function. It has been proposed that LARGE possesses the great potential to rescue glycosylation defects in α-DGPs regardless of causative genes. However, the in vivo therapeutic benefit of using LARGE activity is controversial. To explore the conditions needed for successful LARGE gene therapy, here we used *Large*-deficient and *fukutin*-deficient mouse models for MDC1D and FCMD, respectively. Myofibre-selective LARGE expression via systemic adeno-associated viral gene transfer ameliorated dystrophic pathology of *Large*-deficient mice even when intervention occurred after disease manifestation. However, the same strategy failed to ameliorate the dystrophic phenotype of *fukutin*-conditional knockout mice. Furthermore, forced expression of *Large* in *fukutin*-deficient embryonic stem cells also failed to recover α-DG glycosylation, however coexpression with *fukutin* strongly enhanced α-DG glycosylation. Together, our data demonstrated that fukutin is required for LARGE-dependent rescue of α-DG glycosylation, and thus suggesting new directions for LARGE-utilizing therapy targeted to myofibres.

α-Dystroglycanopathy (α-DGP) is a genetically and clinically heterogeneous group of muscular dystrophy[1,2] for which more than 15 causative genes have been identified[3–21]: *POMT1, POMT2, POMGnT1, fukutin, FKRP, LARGE, ISPD, GTDC2* (*POMGnT2*), *DAG1, TMEM5, B3GALNT2, SGK196* (*POMK*), *B3GNT1* (*B4GAT1*), *GMPPB, DOLK, DPM1, DPM2 and DPM3*. Regardless of the causative gene, α-DGP is characterized by abnormal glycosylation of α-DG, indicating that the disease is associated with defects in the glycosylation pathway for α-DG. α-DG is a cell surface receptor for matrix and synaptic proteins such as laminins, agrin, perlecan, neurexin, and pikachurin[22,23]. A unique *O*-mannosyl glycosylation is required for the ligand-binding activity of α-DG, and abnormal glycosylation leads to reduced ligand-binding activity[24,25]. α-DG also interacts with a transmembrane β-DG, which in turn binds to intracellular dystrophin[23]. Thus, proper glycosylation of α-DG is necessary for the connection between the basement membrane and cytoskeleton. Disruption of this linkage is thought to cause myofibre membrane weakness, leading to disease-predisposing muscle cell necrosis[26]. Although myofibres can regenerate after necrosis, it has been shown that muscle regeneration activity is impaired in α-DGP[27]. Thus, α-DG glycosylation is important for maintenance of skeletal muscle viability and defects in this process underlie the pathogenesis of α-DGP.

α-DGP includes Fukuyama congenital muscular dystrophy (FCMD), muscle-eye-brain disease (MEB), Walker-Warburg syndrome (WWS), and several types of congenital muscular dystrophies (MDCs) and limb-girdle muscular dystrophies (LGMDs)[1,2]. The clinical spectrum of α-DGP is wide; the most severe cases exhibit congenital muscular dystrophy with structural abnormalities in the brain and eyes, whereas the mildest form presents as adult-onset LGMD with no central nervous system involvement[28–30]. In addition, there is no clear genotype-phenotype correlation. Thus, it has been proposed that α-DGPs can be classified into three broad phenotypic groups, MDDG (muscular dystrophy dystroglycanopathy) type A, B and C[29]: MDC with brain/eye abnormalities (A), MDC with milder brain structural abnormalities (B), and LGMD (C). FCMD is the first

identified α-DGP[31] and the second most common childhood muscular dystrophy in Japan[32,33]. The causative gene for FCMD is *fukutin*[6]. *LARGE* was identified as the gene responsible for MDC1D[8]. Fukutin and LARGE are involved in a novel phosphodiester-linked modification, namely, post-phosphoryl modification, of *O*-mannose on α-DG[24,34]. Although the exact function of fukutin is unknown, LARGE was recently shown to be a glycosyltransferase that catalyses the formation of a repeating [-3Xyl-α1,3GlcAβ1-] polymer, which is modified on the distal end of the post-phosphoryl moiety[35]. These repeating units likely serve as the ligand-binding domain of α-DG[36]. Interestingly, overexpression of LARGE causes hyperglycosylation of α-DG with increased ligand-binding activity not only in wild-type and *Large*-deficient muscle cells, but also in cells from WWS, MEB, FCMD patients and mouse models[37]. This finding inspired a novel therapeutic strategy based on the unique activity of LARGE—modulation of LARGE activity can be a versatile treatment for α-DGP, regardless of the causative gene.

After this breakthrough finding, several reports showed that overexpression of LARGE in mice induced hyperglycosylation of α-DG in skeletal muscle of α-DGP mouse models such as *POMGnT1*- and *FKRP*-deficient[38,39]. However, LARGE overexpression in cells lacking GTDC2 expression or POMT1 activity did not induce hyperglycosylation of α-DG[9,40]. Moreover, some studies have shown the beneficial effects of LARGE overexpression in *POMGnT1*- or *FKRP*-mutant mice[38,39], but others showed a deterioration in *FKRP*- or *fukutin*-mutant mice crossed with LARGE-overexpressing transgenic mice[41,42]. Thus, it remains unclear whether LARGE could be a target molecule for α-DGP treatment. We hypothesized that the conditions for LARGE expression such as way of gene delivery, timing of intervention, and target cells may affect α-DG glycosylation and therapeutic consequences. Here, we examined therapeutic benefits of myofibre-selective *Large* gene expression after disease manifestation in *Large*- or *fukutin*-deficient α-DGP mouse models. Our data also showed that fukutin is a prerequisite for LARGE-dependent rescue of α-DG glycosylation.

Results

Myofibre-selective expression of *Large* after disease onset restores α-DG glycosylation and ameliorates dystrophic pathology of *Large^{myd}* mice. We performed systemic *Large* gene delivery after disease manifestation and myofibre-selective *Large* gene expression in α-DGP mouse models. For this purpose, we constructed recombinant adeno-associated virus (AAV) 9 vectors containing the *Large* cDNA under the myofibre-selective muscle creatine kinase (MCK) promoter (AAV9-MCK-*Large*). We first examined the therapeutic benefits of muscle-selective LARGE expression in *Large*-deficient *Large^{myd}* mice. New-born *Large^{myd}* mice (1 week old) showed no signs of muscle pathology (Fig. 1a), but at 4 weeks of age, the *Large^{myd}* skeletal muscles showed signs of muscular dystrophy such as necrotic and regenerating fibres (Fig. 1a). After 4 months, *Large^{myd}* mice showed severe dystrophic pathology in the hind-limb muscles (Fig. 1a). The dystrophic changes include the presence of myofibres with loss of polygonal contour, high population of regenerating fibres with centrally located nuclei, and infiltrations of macrophages and connective tissues. Therefore, we administered intravenous AAV9-MCK-*Large* via the tail vein to 5-week-old *Large^{myd}* mice exhibiting dystrophic symptoms, and then analysed α-DG glycosylation status and therapeutic effects after 5 months. Glycosylation status was evaluated by assessing the reactivity of the monoclonal IIH6 antibody, which recognizes properly glycosylated α-DG[25].

Western blot analysis confirmed LARGE was overexpressed in AAV-treated *Large^{myd}* mice; consequently, the reactivity of IIH6 antibody exceeded even the baseline levels observed in untreated heterozygous animals (Fig. 1b). Immunofluorescence analysis also confirmed increased IIH6-reactivity in the treated *Large^{myd}* skeletal muscles (Fig. 1c). Haematoxylin and eosin (H&E) staining of skeletal muscles indicated decreases in the number of necrotic fibres and recovery of the polygonal contour of myofibres in AAV-treated *Large^{myd}* versus untreated *Large^{myd}* mice (Fig. 1d). The number of muscle fibres with centrally located nuclei as well as infiltration of connective tissues and macrophages were significantly reduced in comparison to the findings obtained for untreated *Large^{myd}* mice (Fig. 2a–c). After the AAV-injection, we tracked changes in grip strength, body weight, and serum creatine kinase (CK). Our results showed significant improvements of these parameters even 4 weeks after the injection (Fig. 2d–f). These results demonstrated that myofibre-selective LARGE expression in *Large^{myd}* mice via systemic administration ameliorates the dystrophic pathology even if the initial intervention occurs after onset.

***Large* gene therapy failed to restore glycosylation and ameliorate muscle pathology of *fukutin*-deficient α-DGP models.** LARGE overexpression increases glycosylation and ligand-binding activity of α-DG in *fukutin*-deficient cells from FCMD patients[37]. We examined whether the muscular dystrophic phenotype of *fukutin*-deficient mice can be improved by LARGE overexpression in vivo. We used muscle precursor cell (MPC)-selective *fukutin*-deficient conditional knock-out (cKO) mice as a *fukutin*-deficient model (Myf5-*fukutin*-cKO mice)[27]. Myf5-*fukutin*-cKO mice showed loss of IIH6-positive glycosylation of α-DG in the skeletal muscles at birth[27]. The dystrophic pathology begins around 4 weeks of age and becomes severe at 12 weeks[27]. We administered intravenous AAV9-MCK-*Large* into 4-week-old Myf5-*fukutin*-cKO mice via the tail vein, and then analysed the glycosylation status of α-DG and therapeutic efficacy after 2 months. Interestingly, although we observed expression of LARGE protein in the AAV-treated Myf5-*fukutin*-cKO skeletal muscles, IIH6-positive α-DG was hardly produced in AAV-treated Myf5-*fukutin* cKO mice (Fig. 3a). Immunofluorescence staining also confirmed failure to restore IIH6-positive glycosylation of α-DG by AAV-treatment in Myf5-*fukutin*-cKO mice (Fig. 3b). H&E staining of skeletal muscles and quantitative muscle pathology showed no significant improvement with AAV treatment (Fig. 3c and Fig. S1a–c). In addition, we found no evidence to support improvements in grip strength, body weight, and serum CK activity after AAV treatment (Fig. S1d–f). These data indicate that the failure to restore α-DG glycosylation in Myf5-*fukutin*-cKO mice is associated with failure of LARGE therapeutic efficacy.

The amount of LARGE protein expressed in the AAV-treated Myf5-*fukutin*-cKO mice was comparable to that in AAV-treated *Large^{myd}* (Fig. 3a). α-DG glycosylation was recovered in *Large^{myd}* skeletal muscle after AAV9-MCK-*Large* treatment, suggesting something other than protein expression levels is responsible for the failure of glycosylation recovery in Myf5-*fukutin*-cKO mice. We hypothesized that complete loss of fukutin caused failure to build the part of post-phosphoryl moiety, which may be required for LARGE-dependent glycosylation; therefore, even excess LARGE protein could not form the [-3Xyl-α1,3GlcAβ1-] polymer on α-DG. To test this hypothesis, we expressed LARGE in *fukutin*-null embryonic stem (ES) cells. Transfection of the *fukutin* cDNA restored IIH6 reactivity in *fukutin*-null ES cells, but transfection of the *Large* cDNA failed to restore α-DG glycosylation, although LARGE expression in wild-type ES cells produced strong IIH6-reactivity (Fig. 4). When the *fukutin* and *Large* cDNAs were co-transfected into *fukutin*-null ES cells, we observed increases in IIH6-reactivity in comparison to *fukutin* singly transfected cells although expression levels of both fukutin and LARGE were much lower than they were in each single transfection (Fig. 4, lanes 6–8). These data show that fukutin-dependent modification is a prerequisite for LARGE-dependent formation of [-3Xyl-α1,3GlcAβ1-] repeating units.

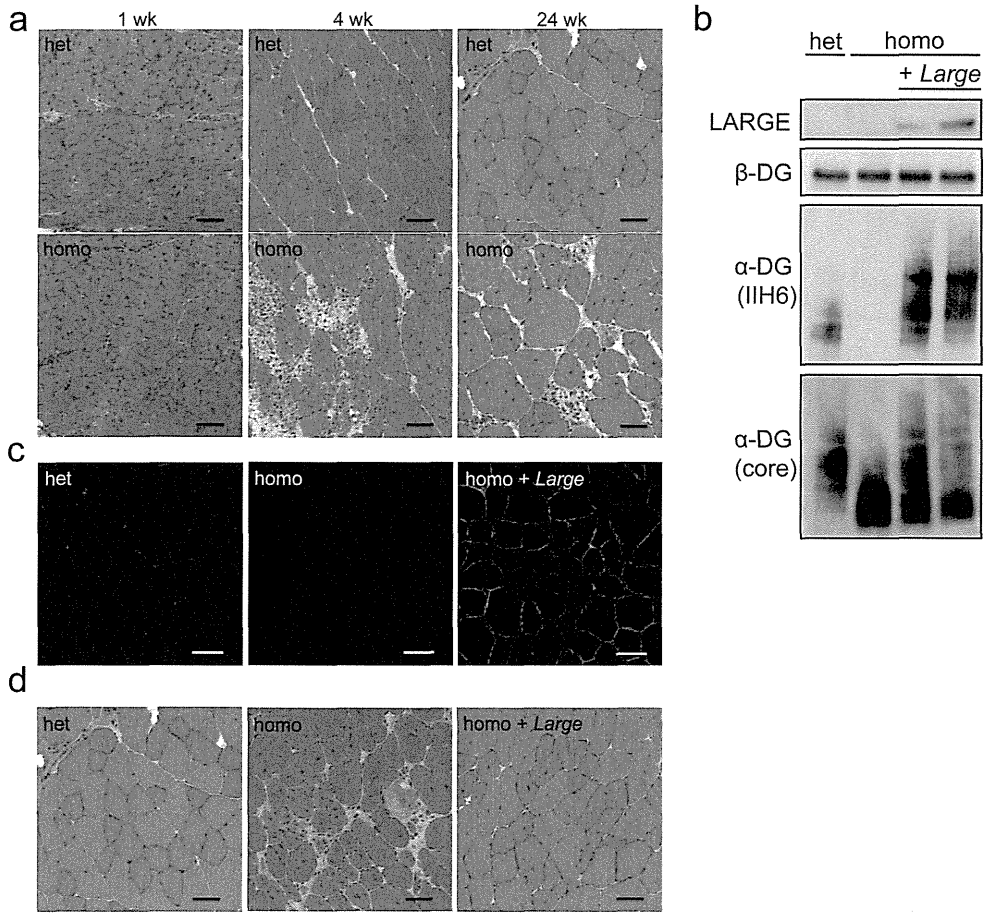

Figure 1 | Systemic gene transfer of *Large* into *Large*^{myd} mice after onset. (a) Histopathological analysis (H&E staining) of the skeletal muscle of *Large*^{myd} (homo) and heterozygous (het) mice at 1, 4, and 24 weeks of age. Bar = 50 μm. (b–d) AAV9-MCK-*Large* was administered to 5-week-old *Large*^{myd} mice via the tail vein; after 5 months, the skeletal muscles were harvested and analysed for α-DG glycosylation (b, c) and histology (d). LARGE was detected by western blotting of total lysates (b). β-DG was used as a loading control. DG proteins enriched with WGA-beads were analysed by western blotting to assess α-DG glycosylation (b). The full-length blots with α-DG (IIH6), α-DG (core), LARGE, and β-DG are presented in Supplementary Figure S2a–d, respectively. Immunofluorescence analysis with IIH6 antibody confirmed the increase in α-DG glycosylation (c). H&E staining of the tibialis anterior muscle indicated amelioration of the muscular dystrophic phenotype after treatment with AAV9-MCK-*Large* (d). Het, *Large*^{myd} heterozygous controls; homo, untreated *Large*^{myd} homozygous mice; and homo + *Large*, *Large*^{myd} homozygous mice with AAV9-MCK-*Large* treatment. Bar = 50 μm.

Discussion

It has been widely recognized that LARGE possesses the great potential to rescue glycosylation defects of α-DG regardless of causative genes for α-DGP, however, therapeutic benefits of using LARGE activity is controversial. To assess the feasibility of LARGE-utilizing therapy, in this study we explored the conditions needed for successful *Large* gene therapy. We demonstrated for the first time that AAV-mediated *Large* gene expression targeted to myofibres is therapeutically beneficial in a *Large*-deficient α-DGP model even when the intervention is performed after disease manifestation. On the other hand, the same strategy failed to restore α-DG glycosylation in *fukutin*-deficient skeletal muscles and ES cells, suggesting that fukutin is required for LARGE-utilizing therapeutic strategy.

Several reports have shown that AAV-mediated LARGE expression, which was driven by the chicken β-actin (CB) promoter, restored glycosylation of α-DG in *Large*^{myd} mice[38,39]. However, expression of exogenous genes by non-selective promoter such as the CB promoter in various non-muscle cells may be detrimental. For example, because glycosylation levels of α-DG and the expression levels of LARGE change during muscle differentiation and regeneration[36], excess glycosylation may disturb cellular homeostasis and tissue regeneration. In fact, LARGE overexpression in C2C12 myoblasts impairs differentiation[42]. Furthermore, there may be situations or cells in which glycosylation is physiologically unnecessary even in wild-type tissues[34]. Although AAV-mediated *Large* gene transfer using the CB promoter rescued the muscular dystrophic phenotype in *Large*^{myd} mice[38,39], this study was designed to introduce viral vectors into new-born pups; thus, it is likely that α-DG restores proper glycosylation before disease manifestation, preventing disease-causing myofibre necrosis. However, in humans, clinical and genetic diagnoses of α-DGP are made after disease manifestation, making gene delivery in new-borns unfeasible. We demonstrated that myofibre-selective expression of LARGE ameliorated the dystrophic phenotype of *Large*^{myd} mice, and the intervention even after disease manifestation was effective by using systemic AAV-mediated gene delivery. The effect continues at least for 5 months after the intervention, the longest period observed in gene therapy studies of α-DGP mouse models. Myofibre-selective rescues of fukutin or LARGE expression by AAV gene transfer or crossing with transgenic mice improved the dystrophic phenotypes of Myf5-*fukutin*-cKO or

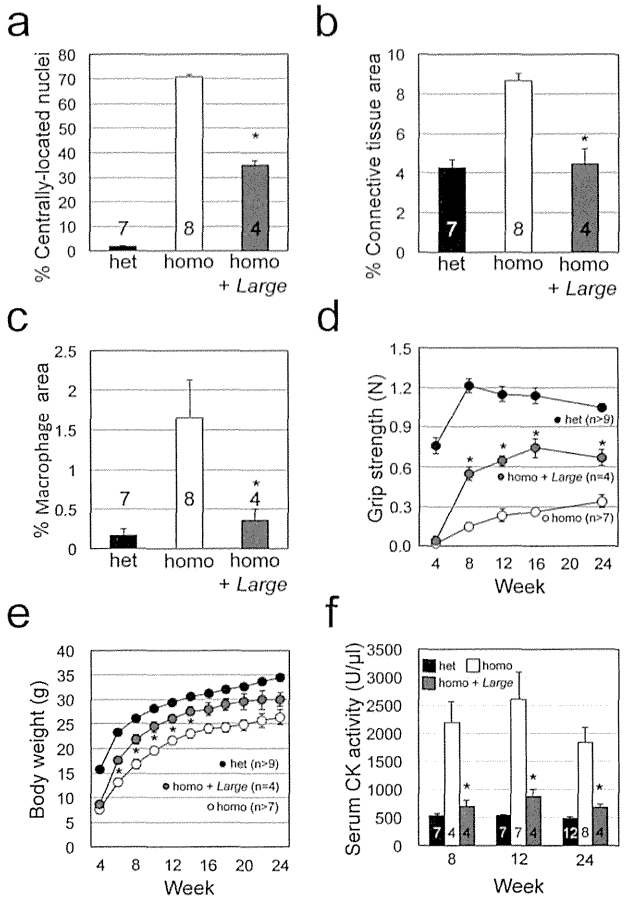

Figure 2 | Quantitative analysis of the therapeutic effects of AAV9-MCK-*Large* treatment in *Large*^{myd} mice. Amelioration of dystrophic histology after AAV9-MCK-*Large* treatment was evaluated by quantifying muscle fibres with centrally located nuclei (a; $P = 0.007$), measuring infiltration of connective tissue by collagen I-immunofluorescence staining (b; $P = 0.007$) and infiltration of macrophages by F4/80-immunofluorescence staining (c; $P = 0.011$). Therapeutic efficacy over time was evaluated by grip strength (d; $P = 0.007$, 0.006, 0.008, and 0.014 for 8, 12, 16, and 24 weeks), body weight (e; $P = 0.019$, 0.019, 0.024, 0.017, and 0.032 for 6, 8, 10, 12, and 14 weeks), and serum CK activity (f; $P = 0.021$, 0.008, and 0.011 for 8, 12, and 24 weeks). Data shown are mean ± s.e.m. for each group (n is indicated in the graph). $*P \leq 0.05$ vs. non-treated *Large*^{myd} homozygous mice (Mann–Whitney U test). Het, *Large*^{myd} heterozygous controls; homo, untreated *Large*^{myd} homozygous mice; and homo + *Large*, *Large*^{myd} homozygous mice with AAV9-MCK-*Large* treatment.

Large^{myd} mice[27,43], supporting the validity of myofibre-selective gene rescue for treatment of α-DGP. We propose that myofibre-targeting rescue/reinforcement of glycosylation is an effective treatment for α-DGP.

We also examined the potential of LARGE as a therapeutic target for *fukutin*-deficient α-DGP; however, our data showed that LARGE expression failed to restore α-DG glycosylation in *fukutin*-null myofibres and ES cells. LARGE synthesises [-3Xyl-α1,3GlcAβ1-] repeating units in the terminal end of the post-phosphoryl moiety, which is modified on phospho-mannose in the Core M3 structure, GalNAc-GlcNAc-Man(P)-O[24,35,44]. The activities of POMT and GTDC2 are required for Core M3 synthesis and fukutin mediates formation of the post-phosphoryl modification[24,34,44]. In cells lacking POMT activity or GTDC2 expression, LARGE overexpression failed to induce hyperglycosylation or restore glycosylation of α-DG[9,40]. Thus, even when overexpressed, LARGE requires the Core M3 structure and fukutin-dependent modification in order to form the [-3Xyl-α1,3GlcAβ1-] repeating units. However, several reports have shown LARGE-dependent glycosylation recovery in genetically distinct α-DGP models[38,39], which seems contradictory but can be explained by the presence of residual glycosylation of α-DG. Presumably, α-DG is hypoglycosylated in such cells, but there might be a small amount of normally glycosylated α-DG species produced by residual activity of the mutant gene products. In fact, the *fukutin*-knock-in and *POMGnT1*-KO mice showed slight reactivity against IIH6 antibody, indicating the presence of normally glycosylated α-DG[45,46]. In such cases, LARGE can reinforce [-3Xyl-α1,3GlcAβ1-] repeats on the small amount of residual Core M3 structure. Importantly, many mild cases of FCMD patients show the presence of a small fraction of normally glycosylated α-DG[30]. Thus, the concept of LARGE modulation therapy remains attractive for a wide range of mild cases of α-DGP such as MDDG type C.

An important issue when considering therapeutic applications is that α-DGP is accompanied by central nervous system abnormalities including severe defects in structural development and mental retardation[28,29]. Although the AAV9 vector delivers genes to central nervous tissues[47], there are many obstacles to treatment for developing central nervous tissues. For example, the structural abnormalities in the central nervous system occur during fetal developing stage[48,49], and such abnormalities are thought to be irreversible after birth. Moreover, fetal therapy also contains many concerns such as ethical, legal, technical, and clinical safety issues. However, improvement of muscle functions via muscle-targeting strategies will improve patients' activities of daily living and caregivers' burdens, and may have an impact on patient mental development. We propose that gene therapy is an effective approach to α-DGP even after disease progression, and that LARGE therapy may be applied to mild cases of α-DGP. Our study will provide a new direction for therapeutic approached to α-DGP.

Methods

Animals. *Large*-deficient *Large*^{myd} mice were from Jackson Laboratories. Generation of muscle precursor cell (MPC)-selective *fukutin* conditional knock-out (cKO) mice (Myf5-*fukutin*-cKO mice) was described previously[27]. All animal procedures were approved by the Animal Care and Use Committee of Kobe University Graduate School of Medicine (P120202-R2) in accordance with the guidelines of the Ministry of Education, Culture, Sports, Science and Technology (MEXT) and the Japan Society for the Promotion of Science (JSPS). The animals were housed in cages (2–4 mice per cage) with wood-chip bedding in an environmentally controlled room (25°C, 12 h light-dark cycle) and provided food and water *ad libitum* at the animal facility of Kobe University Graduate School of Medicine. Well-trained and skilled researchers and experimental technicians, who have knowledge of methods to prevent unnecessary and excessive pain, handled the animals and performed the experiments. Euthanisation was done by cervical dislocation. At sacrifice, the muscles were harvested and snap-frozen in liquid nitrogen (for biochemistry) or in liquid-nitrogen-cooled isopentane (for immunofluorescence and histology). The number and ages of the animals used in each experiment are indicated in the Figure legends and graphs.

Adeno-associated viral gene transfer and evaluation of therapeutic efficacy. To generate a *Large*-encoding AAV9 vector, the complete open reading frame of the mouse *Large* gene was cloned into pAAV-IRES-hrGFP[50]. The MCK promoter was subcloned from AAV-MCKLacZ[51]. The recombinant *Large*-encoding AAV9 vector (AAV9-MCK-*Large*) was produced as described[50]. The AAV9-MCK-*Large* viral vectors (5×10^{11} vector genome) were injected into *Large*^{myd} (n = 4) and Myf5-*fukutin* cKO (n = 6) mice via tail vein at 4–5 weeks of age. Before the injection, body weight, grip strength, and serum CK activity were measured. These clinical parameters (body weight, grip strength, and serum CK activity) were continuously measured until the AAV-treated mice were sacrificed for histological evaluation (the time points of the clinical tests were shown in the figures). The H&E and immunofluorescence images shown in the figures are representative of the AAV-treated and non-treated mice.

Quantitative evaluation of muscle pathology was performed by assessing the number of myofibres with centrally located nuclei at least 1,000 fibres. Macrophage and connective tissue infiltration was quantified by analysing the immunofluorescence signals of F4/80-positive and collagen I-positive areas with Image J software. Serum CK activity was measured with the CPK kit (WAKO). Grip strength was measured for 10 consecutive trials for each mouse using a strength meter (Ohara Ika

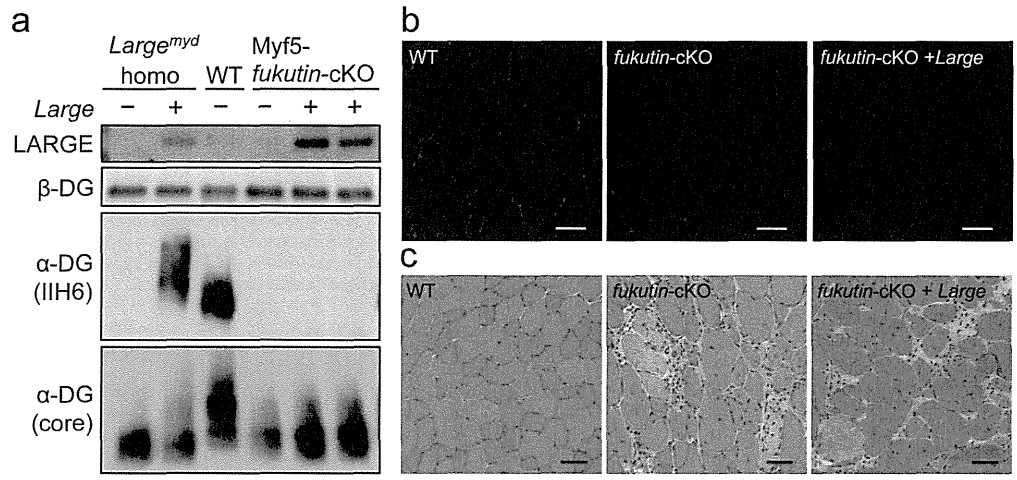

Figure 3 | Systemic gene transfer of *Large* into Myf5-*fukutin* cKO mice after onset. AAV9-MCK-*Large* was administered to 4-week-old Myf5-*fukutin* cKO mice via tail vein injection; after 2 months, the skeletal muscles were harvested and analysed for α-DG glycosylation (a, b) and histology (c). Although LARGE was expressed (a), the levels of α-DG glycosylation were unchanged in AAV-treated Myf5-*fukutin*-cKO mice (a, b). H&E staining for the tibialis anterior muscle did not show improvement of the muscular dystrophic phenotype of Myf5-*fukutin*-cKO mice (c). WT, litter control mice (*fukutin*$^{lox/lox}$ without cre-transgene); *fukutin*-cKO, untreated Myf5-*fukutin*-cKO mice; and *fukutin* cKO + *Large*, Myf5-*fukutin*-cKO mice with AAV9-MCK-*Large* treatment. Bar = 50 μm. The full-length blots with α-DG (IIH6), α-DG (core), LARGE, and β-DG are presented in Supplementary Figure S2e-h, respectively.

Sangyo Co. Ltd., Tokyo); 20% of the top and bottom values were excluded to obtain the mean. Statistical analysis was performed to determine means and s.e.m.; *P*-values <0.05 were considered significant (Mann–Whitney U test).

Antibodies. Antibodies for western blotting and immunofluorescence were as follows: mouse monoclonal antibody 8D5 against β-DG (Novocastra); mouse monoclonal antibody IIH6 against α-DG (Millipore); rat monoclonal antibody against mouse F4/80 (BioLegend); rabbit polyclonal antibody against collagen I (AbD Serotec); mouse monoclonal antibody against FLAG tag (Sigma); and rabbit polyclonal antibody against c-Myc tag (Santa Cruz). Rabbit polyclonal antibody against LARGE was raised using recombinant human LARGE protein expressed in *E. coli*. Antisera were purified by Melon gel IgG purification kit (Pierce). Rat monoclonal antibody against the α-DG core protein (3D7) was generated from a α-DG-Fc fusion protein[52].

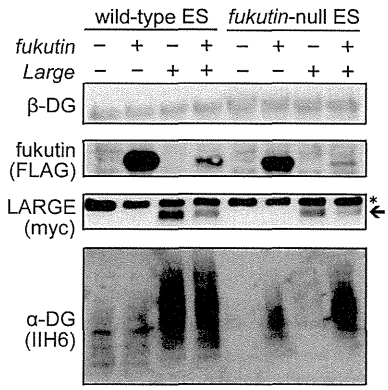

Figure 4 | α-DG glycosylation in *fukutin*-null ES cells after fukutin or LARGE expression. Fukutin (FLAG-tagged) and/or LARGE (myc-tagged) were expressed in wild-type or *fukutin*-null mouse ES cells and α-DG glycosylation status was analysed by western blotting. Exogenous LARGE expression produced highly glycosylated α-DG in wild-type but not *fukutin*-null ES cells, indicated by IIH6 staining. Co-transfection of *fukutin* and *Large* yielded LARGE-dependent glycosylation of α-DG in *fukutin*-null ES cells. Arrow and asterisk indicate LARGE protein and non-specific signals, respectively. The full-length blots with α-DG (IIH6), LARGE (myc), fukutin (FLAG), and β-DG are presented in Supplementary Figure S2i-l, respectively.

Protein preparation and western blotting. DG was enriched from solubilized skeletal muscle as described[27]. Briefly, skeletal muscles (TA ~30 mg, calf ~100 mg) were solubilised in Tris-buffered saline containing 1% Triton X-100 and protease inhibitors (Nacalai). The solubilised fraction was incubated with wheat germ agglutinin (WGA)-agarose beads (Vector Laboratories) at 4°C for 16 h; DG was eluted with SDS-PAGE loading buffer. To detect LARGE protein expression, total lysates were analysed by western blotting. Proteins were separated in 4–15% linear gradient SDS gels, then transferred to polyvinylidene fluoride (PVDF) membranes (Millipore). Blots were probed with antibodies and developed with horseradish peroxidase (HRP)-enhanced chemiluminescence reagent (Supersignal West Pico, Pierce; or ECL Prime, GE Healthcare).

Histology and immunofluorescence analysis. For H&E staining, cryosections (7 μm) were stained for 2 min in haematoxylin, 1 min in eosin, and dehydrated with ethanol and xylene. IIH6-immunofluorescence analysis was performed after treating the with cold ethanol/acetic acid (1 : 1) for 1 min, blocking with 5% goat serum in MOM Mouse Ig Blocking Reagent (Vector Laboratories) at room temperature for 1 h, and incubation with primary antibodies diluted in MOM Diluent (Vector Laboratories) overnight at 4°C. For F4/80- and collagen I-immunofluorescence, sections were blocked with 3% bovine serum albumin (BSA) in phosphate-buffered saline (PBS) at room temperature for 1 h, and then with primary antibodies diluted in 1% BSA overnight at 4°C. The slides were washed with PBS and incubated with Alexa Fluor 488-conjugated or Alexa Fluor 555-conjugated secondary antibodies (Molecular Probes) at room temperature for 30 min. Permount (Fisher Scientific) and TISSU MOUNT (Shiraimatsu Kikai) were used for H&E staining and immunofluorescence, respectively. Sections were observed by fluorescence microscopy (Leica DMR, Leica Microsystems).

ES cell culture. ES cells were cultured in DMEM with 20% heat-inactivated foetal bovine serum, 100 μM 2-mercaptoethanol, 1 mM non-essential amino acids (Gibco), 2 mM L-glutamine (Nacalai), and 10^3 U/mL leukaemia inhibitory factor (Millipore). Targeted disruptions of the *fukutin* gene in ES cells have been described previously[53]. Transfection was performed with Lipofectamine LTX reagents (Invitrogen) according to manufacturer protocols. After 48 h transfection, cells were lysed with Tris-buffered saline containing 1% Triton X-100 and protease inhibitors (Nacalai). DG proteins were enriched with WGA-beads and analysed by western blotting.

1. Toda, T. *et al.* Fukuyama-type congenital muscular dystrophy (FCMD) and alpha-dystroglycanopathy. *Congenit. Anom. (Kyoto).* **43**, 97–104 (2003).
2. Michele, D. E. & Campbell, K. P. Dystrophin-glycoprotein complex: post-translational processing and dystroglycan function. *J. Biol. Chem.* **278**, 15457–15460 (2003).
3. Beltrán-Valero de Bernabé, D. *et al.* Mutations in the O-mannosyltransferase gene POMT1 give rise to the severe neuronal migration disorder Walker-Warburg syndrome. *Am. J. Hum. Genet.* **71**, 1033–1043 (2002).

4. van Reeuwijk, J. *et al.* POMT2 mutations cause alpha-dystroglycan hypoglycosylation and Walker-Warburg syndrome. *J. Med. Genet.* **42**, 907–912 (2005).
5. Yoshida, A. *et al.* Muscular dystrophy and neuronal migration disorder caused by mutations in a glycosyltransferase, POMGnT1. *Dev. Cell* **1**, 717–724 (2001).
6. Kobayashi, K. *et al.* An ancient retrotransposal insertion causes Fukuyama-type congenital muscular dystrophy. *Nature* **394**, 388–392 (1998).
7. Brockington, M. *et al.* Mutations in the fukutin-related protein gene (FKRP) cause a form of congenital muscular dystrophy with secondary laminin alpha2 deficiency and abnormal glycosylation of alpha-dystroglycan. *Am. J. Hum. Genet.* **69**, 1198–1209 (2001).
8. Longman, C. *et al.* Mutations in the human LARGE gene cause MDC1D, a novel form of congenital muscular dystrophy with severe mental retardation and abnormal glycosylation of alpha-dystroglycan. *Hum. Mol. Genet.* **12**, 2853–2861 (2003).
9. Willer, T. *et al.* ISPD loss-of-function mutations disrupt dystroglycan O-mannosylation and cause Walker-Warburg syndrome. *Nat. Genet.* **44**, 575–580 (2012).
10. Roscioli, T. *et al.* Mutations in ISPD cause Walker-Warburg syndrome and defective glycosylation of α-dystroglycan. *Nat. Genet.* **44**, 581–585 (2012).
11. Manzini, M. C. *et al.* Exome sequencing and functional validation in zebrafish identify GTDC2 mutations as a cause of Walker-Warburg syndrome. *Am. J. Hum. Genet.* **91**, 541–517 (2012).
12. Hara, Y. *et al.* A dystroglycan mutation associated with limb-girdle muscular dystrophy. *N. Engl. J. Med.* **364**, 939–946 (2011).
13. Vuillaumier-Barrot, S. *et al.* Identification of mutations in TMEM5 and ISPD as a cause of severe cobblestone lissencephaly. *Am. J. Hum. Genet.* **91**, 1135–1143 (2012).
14. Jae, L. T. *et al.* Deciphering the glycosylome of dystroglycanopathies using haploid screens for lassa virus entry. *Science* **340**, 479–483 (2013).
15. Stevens, E. *et al.* Mutations in B3GALNT2 cause congenital muscular dystrophy and hypoglycosylation of α-dystroglycan. *Am. J. Hum. Genet.* **92**, 354–365 (2013).
16. Buysse, K. *et al.* Missense mutations in β-1,3-N-acetylglucosaminyltransferase 1 (B3GNT1) cause Walker-Warburg syndrome. *Hum. Mol. Genet.* **22**, 1746–1754 (2013).
17. Carss, K. J. *et al.* Mutations in GDP-mannose pyrophosphorylase B cause congenital and limb-girdle muscular dystrophies associated with hypoglycosylation of α-dystroglycan. *Am. J. Hum. Genet.* **93**, 29–41 (2013).
18. Lefeber, D. J. *et al.* Autosomal recessive dilated cardiomyopathy due to DOLK mutations results from abnormal dystroglycan O-mannosylation. *PLoS Genet.* **7**, e1002427 (2011).
19. Yang, A. C. *et al.* Congenital disorder of glycosylation due to DPM1 mutations presenting with dystroglycanopathy-type congenital muscular dystrophy. *Mol. Genet. Metab.* **110**, 345–351 (2013).
20. Barone, R. *et al.* DPM2-CDG: a muscular dystrophy-dystroglycanopathy syndrome with severe epilepsy. *Ann. Neurol.* **72**, 550–558 (2012).
21. Lefeber, D. J. *et al.* Deficiency of Dol-P-Man synthase subunit DPM3 bridges the congenital disorders of glycosylation with the dystroglycanopathies. *Am. J. Hum. Genet.* **85**, 76–86 (2009).
22. Kanagawa, M. Dystroglycan glycosylation and its involvement in muscular dystrophy. *Trends Glycosci. Glycotech.* **26**, 41–57 (2014).
23. Barresi, R. & Campbell, K. P. Dystroglycan: from biosynthesis to pathogenesis of human disease. *J. Cell Sci.* **119**, 199–207 (2006).
24. Yoshida-Moriguchi, T. *et al.* O-mannosyl phosphorylation of alpha-dystroglycan is required for laminin binding. *Science* **327**, 88–92 (2010).
25. Michele, D. E. *et al.* Post-translational disruption of dystroglycan-ligand interactions in congenital muscular dystrophies. *Nature* **418**, 417–422 (2002).
26. Han, R. *et al.* Basal lamina strengthens cell membrane integrity via the laminin G domain-binding motif of alpha-dystroglycan. *Proc. Natl. Acad. Sci. USA.* **106**, 12573–12579 (2009).
27. Kanagawa, M. *et al.* Impaired viability of muscle precursor cells in muscular dystrophy with glycosylation defects and amelioration of its severe phenotype by limited gene expression. *Hum. Mol. Genet.* **22**, 3003–3015 (2013).
28. Godfrey, C. *et al.* Refining genotype phenotype correlations in muscular dystrophies with defective glycosylation of dystroglycan. *Brain* **130**, 2725–2735 (2007).
29. Godfrey, C., Foley, A. R.., Clement, E. & Muntoni, F. Dystroglycanopathies: coming into focus. *Curr. Opin. Genet. Dev.* **21**, 278–285 (2011).
30. Murakami, T. *et al.* Fukutin gene mutations cause dilated cardiomyopathy with minimal muscle weakness. *Ann. Neurol.* **60**, 597–602 (2006).
31. Hayashi, Y. K. *et al.* Selective deficiency of alpha-dystroglycan in Fukuyama-type congenital muscular dystrophy. *Neurology* **57**, 115–121 (2001).
32. Fukuyama, Y., Osawa, M. & Suzuki, H. Congenital progressive muscular dystrophy of the Fukuyama type - clinical, genetic and pathological considerations. *Brain Dev.* **3**, 1–29 (1981).
33. Toda, T., Kobayashi, K., Kondo-Iida, E., Sasaki, J. & Nakamura, Y. The Fukuyama congenital muscular dystrophy story. *Neuromuscul. Disord.* **10**, 153–159 (2000).
34. Kuga, A. *et al.* Absence of post-phosphoryl modification in dystroglycanopathy mouse models and wild-type tissues expressing non-laminin binding form of α-dystroglycan. *J. Biol. Chem.* **287**, 9560–9567 (2012).
35. Inamori, K. *et al.* Dystroglycan function requires xylosyl- and glucuronyltransferase activities of LARGE. *Science* **335**, 93–96 (2012).
36. Goddeeris, M. M. *et al.* LARGE glycans on dystroglycan function as a tunable matrix scaffold to prevent dystrophy. *Nature* **503**, 136–140 (2013).
37. Barresi, R. *et al.* LARGE can functionally bypass alpha-dystroglycan glycosylation defects in distinct congenital muscular dystrophies. *Nat. Med.* **10**, 696–703 (2004).
38. Yu, M. *et al.* Adeno-associated viral-mediated LARGE gene therapy rescues the muscular dystrophic phenotype in mouse models of dystroglycanopathy. *Hum. Gene Ther.* **24**, 317–330 (2013).
39. Vannoy, C. H. *et al.* Adeno-associated virus-mediated overexpression of LARGE rescues α-dystroglycan function in dystrophic mice with mutations in the fukutin-related protein. *Hum. Gene. Ther. Methods.* **25**, 187–196 (2014).
40. Yagi, H. *et al.* AGO61-dependent GlcNAc modification primes the formation of functional glycans on α-dystroglycan. *Sci. Rep.* **3**, 3288 (2013).
41. Whitmore, C. *et al.* The transgenic expression of LARGE exacerbates the muscle phenotype of dystroglycanopathy mice. *Hum. Mol. Genet.* **23**, 1842–1855 (2014).
42. Saito, F. *et al.* Overexpression of LARGE suppresses muscle regeneration via down-regulation of insulin-like growth factor 1 and aggravates muscular dystrophy in mice. *Hum. Mol. Genet.* **23**, 4543–4558 (2014).
43. Gumerson, J. D. *et al.* Muscle-specific expression of LARGE restores neuromuscular transmission deficits in dystrophic LARGE(myd) mice. *Hum. Mol. Genet.* **22**, 757–768 (2013).
44. Yoshida-Moriguchi, T. *et al.* SGK196 is a glycosylation-specific O-mannose kinase required for dystroglycan function. *Science* **341**, 896–899 (2013).
45. Taniguchi-Ikeda, M. *et al.* Pathogenic exon-trapping by SVA retrotransposon and rescue in Fukuyama muscular dystrophy. *Nature* **478**, 127–131 (2011).
46. Kanagawa, M. *et al.* Residual laminin-binding activity and enhanced dystroglycan glycosylation by LARGE in novel model mice to dystroglycanopathy. *Hum. Mol. Genet.* **18**, 621–631 (2009).
47. Foust, K. D. *et al.* Intravascular AAV9 preferentially targets neonatal neurons and adult astrocytes. *Nat. Biotechnol.* **27**, 59–65 (2009).
48. Nakano, I., Funahashi, M., Takada, K. & Toda, T. Are breaches in the glia limitans the primary cause of the micropolygyria in Fukuyama-type congenital muscular dystrophy (FCMD)? Pathological study of the cerebral cortex of an FCMD fetus. *Acta. Neuropathol.* **91**, 313–321 (1996).
49. Chiyonobu, T. *et al.* Effects of fukutin deficiency in the developing mouse brain. *Neuromuscul. Disord.* **15**, 416–426 (2005).
50. Okada, T. *et al.* Scalable purification of adeno-associated virus serotype 1 (AAV1) and AAV8 vectors, using dual ion-exchange adsorptive membranes. *Hum. Gene Ther.* **20**, 1013–1021 (2009).
51. Yuasa, K. *et al.* Adeno-associated virus vector-mediated gene transfer into dystrophin-deficient skeletal muscles evokes enhanced immune response against the transgene product. *Gene Ther.* **9**, 1576–1588 (2002).
52. Kanagawa, M. *et al.* Post-translational maturation of dystroglycan is necessary for pikachurin binding and ribbon synaptic localization. *J. Biol. Chem.* **285**, 31208–31216 (2010).
53. Takeda, S. *et al.* Fukutin is required for maintenance of muscle integrity, cortical histiogenesis and normal eye development. *Hum. Mol. Genet.* **12**, 1449–1459 (2003).

Acknowledgments

We would like to thank the past and present members of Dr. Toda's laboratory for fruitful discussions and scientific contributions. We also thank Hiromi Hayashita-Kinoh for providing technical support. This work was supported by the Ministry of Health, Labour, and Welfare of Japan [Intramural Research Grant for Neurological and Psychiatric Disorders of National Centre of Neurology and Psychiatry (26-8)]; the Ministry of Education, Culture, Sports, Science and Technology of Japan [a Grant-in-Aid for Scientific Research (A) 26253057 to T.T.; a Grant-in-Aid for Young Scientists (A) 24687017 to M.K.; and a Grant-in-Aid for Scientific Research on Innovative Areas (Deciphering sugar chain-based signals regulating integrative neuronal functions) 24110508 to M.K.]; a Senri Life Science Foundation grant to M.K.; and a Takeda Science Foundation grant to M.K.

Author contributions

Y.O., M.K., T.O., K.K., S.T. and T.T. conceived and designed the research. Y.O., M.K. and C.I. performed experiments and analysed the data. C.Y., K.K., T.C. and T.O. constructed the AAV vectors. Y.O., M.K. and T.T. wrote the paper. All authors reviewed the manuscript.

Additional information

Supplementary information accompanies this paper at http://www.nature.com/scientificreports

Competing financial interests: The authors declare no competing financial interests.

How to cite this article: Ohtsuka, Y. *et al.* Fukutin is prerequisite to ameliorate muscular dystrophic phenotype by myofiber-selective LARGE expression. *Sci. Rep.* **5**, 8316; DOI:10.1038/srep08316 (2015).

THE JOURNAL OF BIOLOGICAL CHEMISTRY VOL. 290, NO. 3, pp. 1442–1453, January 16, 2015

p62 Plays a Protective Role in the Autophagic Degradation of Polyglutamine Protein Oligomers in Polyglutamine Disease Model Flies*

Received for publication, June 20, 2014, and in revised form, November 26, 2014 Published, JBC Papers in Press, December 5, 2014, DOI 10.1074/jbc.M114.590281

Yuji Saitoh[‡§¶], Nobuhiro Fujikake[‡], Yuma Okamoto[‡], H. Akiko Popiel[‡], Yusuke Hatanaka[‡], Morio Ueyama[‡], Mari Suzuki[‡], Sébastien Gaumer[‖], Miho Murata[§¶], Keiji Wada[‡], and Yoshitaka Nagai[‡1]**

*From the [‡]Department of Degenerative Neurological Diseases, National Institute of Neuroscience, National Center of Neurology and Psychiatry, 4-1-1 Ogawa-Higashi, Kodaira, Tokyo 187-8502, Japan, the [§]Department of Neurology, National Center Hospital, National Center of Neurology and Psychiatry, 4-1-1 Ogawa-higashi, Kodaira, Tokyo 187-8551, Japan, the [¶]Graduate School of Medical and Pharmaceutical Sciences, Chiba University, 1-8-1, Inohana, Chuo-ku, Chiba, Chiba 260-8670, Japan, the [‖]Laboratoire de Génétique et Biologie Cellulaire, EA4589, Université de Versailles-Saint-Quentin-en-Yvelines, École Pratique des Hautes Etudes, 45 Avenue des Etats-Unis, 78035 Versailles Cedex, France, and **Core Research for Evolutional Science and Technology (CREST), Japan Science and Technology Agency, Kawaguchi, Saitama 332-0012, Japan*

Background: Oligomers of pathogenic proteins are implicated in the pathomechanisms of neurodegenerative diseases.
Results: Depletion of p62 delays the degradation of polyglutamine protein oligomers via autophagy and exacerbates neurodegeneration in polyglutamine disease model flies.
Conclusion: p62 plays a protective role via autophagic degradation of polyglutamine protein oligomers.
Significance: p62 should be a therapeutic target for the polyglutamine diseases.

Oligomer formation and accumulation of pathogenic proteins are key events in the pathomechanisms of many neurodegenerative diseases, such as Alzheimer disease, ALS, and the polyglutamine (polyQ) diseases. The autophagy-lysosome degradation system may have therapeutic potential against these diseases because it can degrade even large oligomers. Although p62/sequestosome 1 plays a physiological role in selective autophagy of ubiquitinated proteins, whether p62 recognizes and degrades pathogenic proteins in neurodegenerative diseases has remained unclear. In this study, to elucidate the role of p62 in such pathogenic conditions *in vivo*, we used *Drosophila* models of neurodegenerative diseases. We found that p62 predominantly co-localizes with cytoplasmic polyQ protein aggregates in the MJDtr-Q78 polyQ disease model flies. Loss of p62 function resulted in significant exacerbation of eye degeneration in these flies. Immunohistochemical analyses revealed enhanced accumulation of cytoplasmic aggregates by *p62* knockdown in the MJDtr-Q78 flies, similarly to knockdown of autophagy-related genes (*Atgs*). Knockdown of both *p62* and *Atgs* did not show any additive effects in the MJDtr-Q78 flies, implying that p62 function is mediated by autophagy. Biochemical analyses showed that loss of p62 function delays the degradation of the MJDtr-Q78 protein, especially its oligomeric species. We also found that loss of p62 function exacerbates eye degeneration in another polyQ disease fly model as well as in ALS model flies. We therefore conclude that p62 plays a protective role against polyQ-induced neurodegeneration, by the autophagic degradation of polyQ protein oligomers *in vivo*, indicating its therapeutic potential for the polyQ diseases and possibly for other neurodegenerative diseases.

The polyglutamine (polyQ)[2] diseases are inherited intractable neurodegenerative diseases, including Huntington disease, several spinocerebellar ataxias (SCA1, -2, -6, -7, and -17 and SCA3/MJD), dentatorubral-pallidoluysian atrophy, and spinobulbar muscular atrophy, which are caused by the expansion of a CAG repeat encoding for polyQ stretch within specific genes (1). PolyQ proteins are prone to misfold, oligomerize, and form aggregates and eventually accumulate as inclusion bodies in affected neurons (2, 3). Whereas the formation of polyQ protein inclusion bodies is believed to be protective, by sequestering the toxic polyQ proteins (4), the intermediate structures formed during the aggregation process, such as monomers or oligomers, are reported to be more toxic for the cells, leading to neuronal dysfunction or neuronal cell death (5, 6). The polyQ diseases are thus considered as one of the protein-folding diseases, together with Alzheimer disease, Parkinson disease, and ALS. Because there are currently no effective therapies for the polyQ diseases, establishment of a novel therapy based on the

* This work was supported in part by Grants-in-Aid for Scientific Research (B) (to Y. N.) from the Japan Society for the Promotion of Science (JSPS), Japan; by Grants-in-Aid for Scientific Research on Priority Areas (Proteolysis) (to Y. N.) and on Innovative Areas (Synapse and Neurocircuit Pathology) (to Y. N.) from the Ministry of Education, Culture, Sports, Science, and Technology, Japan; by Health Labor Sciences Research Grants for Research on Development of New Drugs and the Research Committee for Ataxic Diseases (to Y. N.) from the Ministry of Health, Labor, and Welfare, Japan; and by a grant from Core Research for Evolutional Science and Technology (CREST) of the Japan Science and Technology Agency (to Y. N.).

[1] To whom correspondence should be addressed: Dept. of Degenerative Neurological Diseases, National Institute of Neuroscience, National Center of Neurology and Psychiatry, 4-1-1 Ogawa-Higashi, Kodaira, Tokyo 187-8502, Japan. Tel.: 81-42-346-1715; Fax 81-42-346-1745; E-mail: nagai@ncnp.go.jp.

[2] The abbreviations used are: polyQ, polyglutamine; UPS, ubiquitin-proteasome system; MJDtr, truncated form of mutant MJD; IR, inverted repeat RNA; Aβ, amyloid-β; AGE, agarose gel electrophoresis; SEM, scanning electron microscopic.

disease pathomechanism is a challenging theme. Considering the pathomechanism of the polyQ diseases, the clearance of toxic forms of the polyQ proteins should be a promising therapeutic strategy.

Although the precise mechanisms of how polyQ proteins are degraded in the cell are not clearly understood, the two major cellular degradation systems (*i.e.* the autophagy-lysosome system and the ubiquitin-proteasome system (UPS)) are both thought to be involved in polyQ protein degradation (7). However, the UPS may be inadequate for degrading polyQ protein oligomers or aggregates, because substrate proteins of the UPS need to be unfolded when entering the narrow proteasomal pore (8). Furthermore, the mammalian UPS might not have a protease activity to efficiently degrade the polyQ stretch (9, 10). Alternatively, autophagy can degrade even large aggregates by sequestering and delivering them to the lysosome (11). Although autophagy was considered a non-selective degradation system in the past, emerging evidence suggests that it can specifically degrade some ubiquitinated proteins, organelles, and intracellular pathogens; this is now known as "selective autophagy" (12). The specific autophagic degradation of polyQ proteins, including large sized aggregates, would be a preferable therapeutic strategy, because nonspecific degradation of cytosolic proteins may cause adverse effects due to the loss of normal protein functions.

The p62/sequestosome 1 protein (hereafter called p62) was initially identified as an adaptor molecule for the selective autophagic degradation of ubiquitinated proteins, because p62 has domains that bind both ubiquitinated proteins and autophagosomes, giving selectivity to autophagy (13, 14). Neuropathological studies revealed that p62 co-localizes with ubiquitin-positive inclusions consisting of disease-causative proteins within neurons and glia of patients with various neurodegenerative diseases (15, 16). This evidence suggests that p62 is associated with various abnormal proteins, including the polyQ protein. However, whether p62 recognizes these pathogenic proteins as substrates for p62-associated selective autophagy has remained unclear.

In this study, we explored the role of p62 in the polyQ diseases, using *Drosophila* polyQ disease models. We demonstrated that p62 plays an important role in the autophagic degradation of polyQ protein oligomers, resulting in protection against polyQ protein toxicity *in vivo*. Furthermore, we demonstrated the protective role of p62 in various neurodegenerative disease models, indicating that p62 could be a therapeutic target for various neurodegenerative diseases.

EXPERIMENTAL PROCEDURES

Fly Stocks—Flies were raised and maintained on standard cornmeal-agar-yeast-based food at 25 °C. The transgenic fly lines bearing the *gmr-GAL4* (17) or *UAS*-human *TDP-43*[3] transgene have been described previously. The transgenic fly lines bearing the *gmr-GeneSwitch* or *gmr-grim* transgene and the mutant fly line bearing the $Atg6^{00096}$ mutation were obtained from the Bloomington *Drosophila* Stock Center. The transgenic fly lines bearing the *UAS-MJDtr-Q78* and *UAS-MJDtr-Q27* transgene were gifts from Drs. N. M. Bonini (18), and the *UAS-Httex1p97QP* (19), *UAS-Aβ arc2* (20), and *UAS-R406W tau* (21) transgene were gifts from J. L. Marsh, D. C. Crowther, and M. B. Feany, respectively. The mutant fly lines bearing a *ref(2)P* mutation, namely $ref(2)P^{od2}$ or $ref(2)P^{od3}$, were described previously (22). The RNAi fly lines bearing the *UAS-ref(2)P-IR*, *UAS-Atg12-IR*, *UAS-alfy-IR*, or *UAS-Prosβ2-IR* transgene were obtained from the Vienna *Drosophila* Resource Center.

Fly Eye Imaging—Light microscopic images were taken using a stereoscopic microscope model SZX10 (Olympus, Tokyo, Japan) with a CCD camera (PD21, Olympus, Tokyo, Japan). Scanning electron microscopic (SEM) images were taken using an electron microscope (model TM1000, Hitachi, Tokyo, Japan).

Calculation of Eye Pigmentation Score—The eye images of adult flies were obtained. To quantitatively evaluate the degree of eye degeneration in the MJDtr-Q78 flies, the area of remaining normal pigment in their eyes were measured using the National Institutes of Health ImageJ software as follows: 1) extraction of the green color to produce grayscale images and determination of the area of compound eye as the region of interest (Fig. 2, *Q* and *R*); 2) smoothing of the images by Gaussian blur (Fig. 2*S*), production of binary images, and adjustment of the threshold of the binary images to determine the area of remaining normal pigment in the eyes (Fig. 2*T*); and 3) calculation of the mean area of remaining normal pigment within the region of interest. For the TDP-43 flies, the region of interest was determined in the anterior half of the eye to avoid the necrotic tissues appeared in the posterior half because the necrotic tissues could be misjudged as normal pigment. More than four eyes were analyzed in each experiment.

Calculation of the Number of Interommatidial Bristles—The SEM images of adult fly eyes were obtained. The number of interommatidial bristles within a 150-μm^2 area in the eye was counted (23). Seven eyes were analyzed in each genotype.

Calculation of Eye Size—The light microscopic images of adult fly eyes were obtained. The eye size was measured using ImageJ software (24). Ten eyes were analyzed in each genotype.

Immunohistochemistry—Eye discs were dissected from third instar larvae, fixed with 4% paraformaldehyde, and then immunostained with a rat monoclonal anti-HA antibody (clone 3F10, Roche Applied Science), a rabbit polyclonal anti-Ref(2)P/p62 protein antibody (22), or a mouse monoclonal anti-elav antibody (clone 9F8A9, Developmental Studies Hybridoma Bank, Iowa City, IA) at 1:200 dilution as the primary antibody. As the secondary antibody, an Alexa 568-conjugated anti-rat antibody, an Alexa 488-conjugated anti-rabbit antibody, or an Alexa 488-conjugated anti-mouse antibody was used at 1:1000 dilution. Nuclei were stained using DAPI (Bio-Rad) after the secondary antibody staining. An Alexa 647-conjugated wheat germ agglutinin (Molecular Probes, Inc., Eugene, OR) staining to define the nuclear membrane was performed after DAPI staining at 1:500 dilution. Images were then taken by confocal laser-scanning microscopy (FV1000, Olympus, Tokyo, Japan).

[3] N. Fujikake, N. Kimura, Y. Saitoh, S. Nagano, Y. Hatanaka, T. Ishiguro, T. Takeuchi, M. Suzuki, H. A. Popiel, E. N. Minakawa, M. Ueyama, G. Matsumoto, A. Yokoseki, N. Nukina, T. Araki, O. Onodera, K. Wada, and Y. Nagai, submitted for publication.

The number of MJDtr-Q78 protein aggregates in the eye discs was quantitatively measured using the FV10-ASW 2.0 Viewer software (Olympus, Tokyo, Japan), as follows: 1) selection of photoreceptor neurons within the 13 developing ommatidia in row 2 and row 3 at the posterior tip of the eye discs, by anti-elav staining (Fig. 4, *E* and *F*), because these ommatidia are in approximately the same developing stage and can be easily identified; 2) counting of the number of MJDtr-Q78 protein aggregates localized in either the cytoplasm or the nucleus, judged by whether they merge with the nuclei stained with DAPI or not (Fig. 4, *G* and *H*). More than five eye discs were analyzed in each experiment.

Western Blot Analysis—Five heads of adult flies or 20 eye discs of larvae were lysed in 100 μl of SDS sample buffer using a pestle, sonicated, boiled for 5 min, and centrifuged at 10,000 × *g* for 3 min at 25 °C. The supernatants were run on a 5–20% gradient polyacrylamide gel (Wako, Osaka, Japan) and then transferred onto an Immun-Blot PVDF membrane (Bio-Rad). The membrane was blocked with 5% skim milk in PBS containing 0.1% Tween 20 for 30 min at room temperature and then incubated overnight with a rat monoclonal anti-HA antibody (clone 3F10, Roche Applied Science), a rabbit polyclonal anti-Ref(2)P/p62 antibody (22), or a mouse monoclonal anti-actin antibody (clone AC-40, Sigma-Aldrich) at 1:1000 dilution as primary antibody. After overnight incubation, the membranes were incubated with HRP-conjugated secondary antibodies. Membranes were then treated with SuperSignal West Dura chemiluminescent substrate (Thermo Fisher Scientific), and images were taken by the LAS-4000 imaging system (Fujifilm, Tokyo, Japan). Quantification of each signal was performed using the MultiGauge software (Fujifilm).

SDS-Agarose Gel Electrophoresis (SDS-AGE)—SDS-AGE was performed according to the previous reports (25–27). Briefly, adult fly head lysates were run on a 1.5% agarose, 0.1% SDS gel and then transferred onto a nitrocellulose membrane (Schleicher & Schuell BioScience). Blocking with skim milk, reaction with the primary or secondary antibody, and detection were done with the same protocols as Western blot analysis.

Gene Switch Protocol—RU486 (mifepristone, Sigma-Aldrich) was dissolved in 100% ethanol, further diluted in water, and then mixed with Instant *Drosophila* medium at a final concentration of 10 μg/ml (Carolina Biological Supply Company, Burlington, NC). For RU486 treatment, flies were in RU486-containing medium from the larval stage until adulthood.

Statistical Analyses—For comparisons between two groups, statistical differences were analyzed by Student's *t* test. Data are presented as the mean ± S.E. A *p* value of <0.05 was considered to indicate a statistically significant difference between groups.

RESULTS

p62 Co-localizes with Cytoplasmic PolyQ Protein Aggregates—To evaluate whether p62 affects the polyQ protein *in vivo*, we used the MJDtr-Q78S transgenic fly line, which expresses a truncated form of the mutant MJD protein with an expanded Gln-78 repeat (MJDtr-Q78). As a control, we used the MJDtr-Q27 transgenic fly line, which expresses a truncated form of the MJD protein with a normal-length Gln-27 repeat (MJDtr-Q27). The MJDtr-Q78S flies showed severe compound eye degeneration when the MJDtr-Q78 protein was selectively expressed in the eye by the *gmr-GAL4* driver, as revealed by light microscopic analyses (18) (Fig. 1*B*). On the contrary, the MJDtr-Q27 flies did not show any eye degenerative phenotypes (Fig. 1*A*). In these MJDtr-Q78S flies, the MJDtr-Q78 protein was found to accumulate as aggregates in both the cytoplasm and nucleus, although nuclear aggregates were more abundant than cytoplasmic aggregates (Fig. 1, *I* and *J*). To evaluate the relationship between p62 and the MJDtr-Q78 protein, we performed immunohistochemical analyses of larval eye discs. In the MJDtr-Q27 flies, p62 was predominantly present in the cytoplasm (Fig. 1, *C–H*), and punctate dotlike structures were also observed, which are known as "p62 bodies" (28) (Fig. 1*F*, *open arrows*). On the other hand, in the MJDtr-Q78S flies, p62 co-localized with cytoplasmic MJDtr-Q78 protein aggregates but not with nuclear aggregates (Fig. 1, *I–N*), although most MJDtr-Q78 protein aggregates were present in the nucleus. Wheat germ agglutinin staining to define the nuclear membrane revealed that p62-positive MJDtr-Q78 protein aggregates are present in the cytoplasm, and p62-negative MJDtr-Q78 protein aggregates are present in the nucleus (Fig. 1, *O–Q*). The size of p62-positive MJDtr-Q78 protein aggregates was much larger than that of the p62 bodies seen in the control flies, indicating that these p62-positive MJDtr-Q78 protein aggregates are different from the p62 bodies (Fig. 1, *F* and *L*). These results suggest that p62 is associated with the MJDtr-Q78 protein, especially with its cytoplasmic aggregates.

Loss of p62 Function Causes Exacerbation of Eye Degeneration in PolyQ Disease Model Flies—To evaluate the role of p62 in the pathomechanisms of the polyQ disease model flies, we examined the effect of the loss of p62 function on eye degeneration in two different MJDtr-Q78 fly lines: MJDtr-Q78S and MJDtr-Q78W flies. The latter flies express a lower expression level of the MJDtr-Q78 protein and show milder eye degeneration than the MJDtr-Q78S flies (Fig. 2, *A*, *B*, *E*, and *I*). We used a transgenic RNAi fly line that expresses an inverted repeat RNA (IR) of *ref(2)P*, the *Drosophila* ortholog of the *p62* gene, and two different mutant fly lines of *p62*: *ref(2)P*^{od2}, bearing a deletion of the Phox and Bem1p (PB1) domain, and *ref(2)P*^{od3}, bearing a deletion of the ubiquitin-associated domain (22). We confirmed the efficient knockdown of p62 protein expression when p62-IR is expressed throughout the whole fly body by the *tub-GAL4* driver (Fig. 2, *C* and *D*). When we crossed the MJDtr-Q78S flies with the p62-IR flies or *p62* mutant flies, we found that *p62* knockdown or *p62* mutations significantly aggravate the compound eye degeneration of the MJDtr-Q78S flies, resulting in more severe depigmentation and the appearance of necrotic tissue (Fig. 2, *E–H*). Knockdown of *p62* caused more severe eye degeneration than *p62* mutations, probably because *p62* mutant flies also possess a wild-type *p62* allele in *trans* to the mutant allele. Next, we examined the effect of loss of p62 function in the MJDtr-Q78W fly line. Knockdown of *p62* or *p62* mutations caused the exacerbation of eye depigmentation (Fig. 2, *I–L*), suggesting a protective role of p62 against polyQ-induced eye degeneration. Upon quantification of the eye pigmentation by imaging analyses (Fig. 2, *Q–T*), the exacerbation of eye depigmentation by *p62* knockdown or *p62* mutations was statistically significant (Fig. 2*U*). The exacerbation by loss of

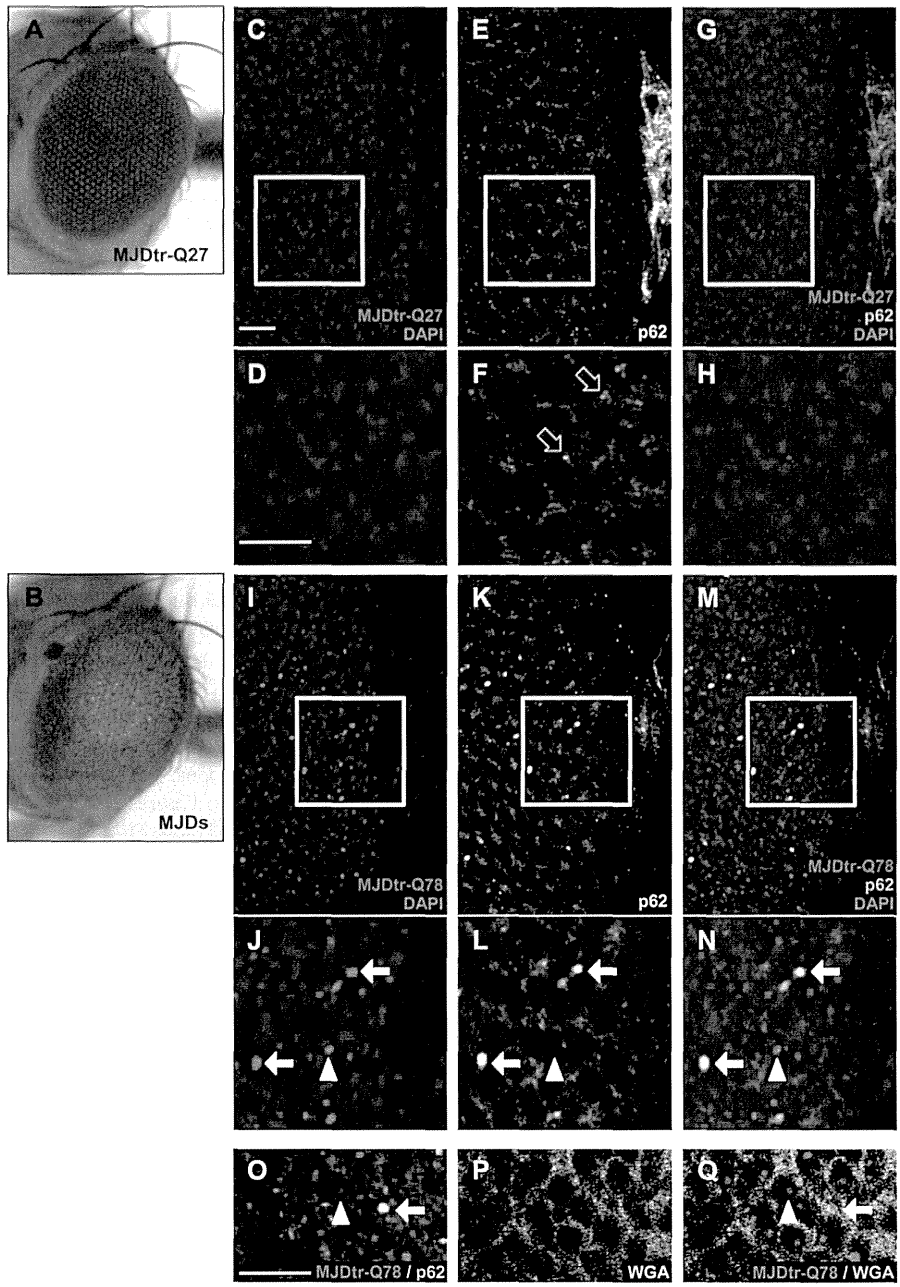

FIGURE 1. **p62 co-localizes with cytoplasmic aggregates of the MJDtr-Q78 protein.** *A* and *B*, light microscopic images of the external compound eyes of the control 1-day-old adult MJDtr-Q27 flies (*A*) and MJDtr-Q78S flies (*MJDs*) (*B*). *C–N*, confocal microscopic images of the larval eye discs of the control MJDtr-Q27 flies (*C–H*) and MJDtr-Q78S flies (*I–Q*), stained with an anti-HA antibody to detect the MJDtr-Q27 or MJDtr-Q78 protein (*red*), an anti-Ref(2)P/p62 antibody (*white* in *E*, *F*, *K*, and *L* and *green* in *G*, *H*, *M*, *N*, and *O*), DAPI for nuclear staining (*blue*), and wheat germ agglutinin to define the nuclear membrane (*white* in *P* and *green* in *Q*). *D*, *F*, *H*, *J*, *L*, and *N*, high magnification images of the indicated areas of *C*, *E*, *G*, *I*, *K*, and *M*, respectively. The *white arrows* and *arrowheads* indicate cytoplasmic and nuclear MJDtr-Q78 protein aggregates, respectively, and the *open arrows* indicate punctate dotlike structures of p62. *Bars*, 10 μm. Fly genotypes were as follows: *gmr-GAL4/+;;UAS-MJDtr-Q27/+* (*A* and *C–H*) and *gmr-GAL4/+;UAS-MJDtr-Q78S/+* (*B* and *I–Q*).

p62 function became even more evident upon the age-related progression of eye degeneration (Fig. 3). We confirmed that either *p62* knockdown or *p62* mutation does not cause any deleterious effects on the eyes of the flies expressing the MJDtr-Q27 protein (Fig. 2, *M–P* and *V*) or expressing the GAL4 protein alone (data not shown), excluding the possibility that the exacerbation of eye degeneration could be a simple additive effect. Furthermore, to exclude the possibility that p62 generally affects any degeneration regardless of the cause, we examined the effect of *p62* knockdown on the flies expressing Grim, which causes eye degeneration by apoptosis (Fig. 2*W*). We found that eye degeneration in the *grim* flies is not affected by *p62* knockdown (Fig. 2, *W–Y*), suggesting that the protective role of p62 is specific to polyQ protein toxicity.

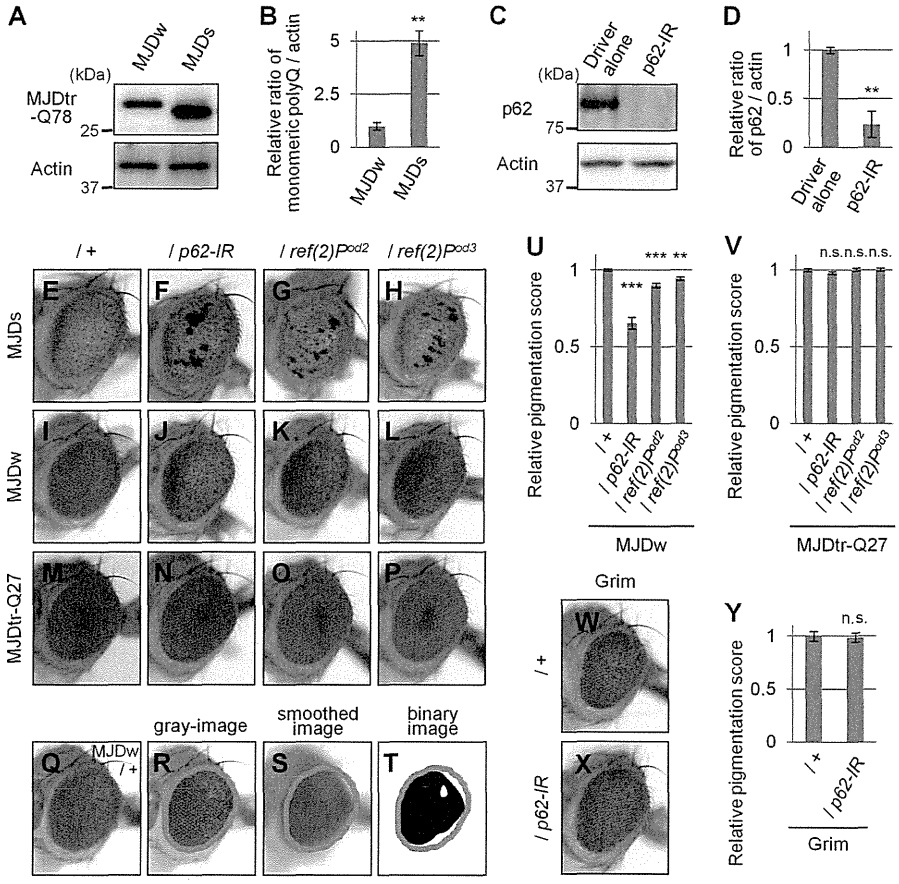

FIGURE 2. **Loss of p62 function causes exacerbation of eye degeneration in MJDtr-Q78 flies.** *A* and *B*, Western blot analysis of the monomeric MJDtr-Q78 protein in larval eye disc lysates of the MJDtr-Q78S flies (*MJDs*) and the MJDtr-Q78W (*MJDw*) flies expressing the MJDtr-Q78 protein under the *gmr-GAL4* driver, using an anti-HA antibody to detect the MJDtr-Q78 protein. The expression level of actin was used as a protein-loading control. The graph shows the relative ratio of the MJDtr-Q78 protein to actin. The relative amount of each protein was measured by densitometric analysis of the bands in *A*. Data are presented as the mean ± S.E. (**, $p < 0.01$, *versus* the MJDw flies) ($n = 3$). Fly genotypes were *gmr-GAL4/+;;UAS-MJDtr-Q78W/+* and *gmr-GAL4/+;UAS-MJDtr-Q78S/+*. *C* and *D*, knockdown efficiency of RNAi-mediated knockdown of *ref(2)P*, the *Drosophila* ortholog of the *p62* gene. The p62 protein in lysates prepared from adult fly heads expressing an IR targeted to *ref(2)P/p62* under the *tub-GAL4* driver was detected with the anti-Ref(2)P/p62 antibody by Western blot analysis. The expression level of actin was used as a protein-loading control. The graph shows the relative ratio of p62 protein to actin. The relative amount of each protein was measured by densitometric analyses of the bands in *C*. Data are presented as the mean ± S.E. (**, $p < 0.01$, *versus* the control flies expressing the GAL4 protein alone) ($n = 3$). Fly genotypes were *tub-GAL4/+* and *UAS-p62-IR/+;tub-GAL4/+*. *E–P*, light microscopic images of the external compound eyes of 1-day-old adult flies of two different MJDtr-Q78 fly lines, MJDtr-Q78S flies (*E*, *MJDs*) and MJDtr-Q78W flies (*I*, *MJDw*), expressing p62-IR (*F* and *J*) or bearing *p62* mutations, namely, *ref(2)P^{od2}* (*G* and *K*) and *ref(2)P^{od3}* (*H* and *L*), and the control MJDtr-Q27 flies (*M–P*). Note that the *p62* mutant flies also possess a wild-type *p62* allelle in *trans* to the mutant allele. Fly genotypes were as follows: *gmr-GAL4/+;UAS-MJDtr-Q78S/+* (*E*); *gmr-GAL4/+;UAS-MJDtr-Q78S/UAS-p62-IR* (*F*); *gmr-GAL4/+;UAS-MJDtr-Q78S/ref(2)P^{od2}* (*G*); *gmr-GAL4/+;UAS-MJDtr-Q78S/ref(2)P^{od3}* (*H*); *gmr-GAL4/+;;UAS-MJDtr-Q78W/+* (*I*); *gmr-GAL4/+;UAS-p62-IR/+;UAS-MJDtr-Q78W/+* (*J*); *gmr-GAL4/+;ref(2)P^{od2}/+;UAS-MJDtr-Q78W/+* (*K*); *gmr-GAL4/+;ref(2)P$^{od3/+}$UAS-MJDtr-Q78W/+* (*L*); *gmr-GAL4/+;;UAS-MJDtr-Q27/+* (*M*); *gmr-GAL4/+;UAS-p62-IR/+;UAS-MJDtr-Q27/+* (*N*); *gmr-GAL4/+;ref(2)P^{od2}/+;UAS-MJDtr-Q27/+* (*O*); and *gmr-GAL4/+;ref(2)P^{od3}/+;UAS-MJDtr-Q27/+* (*P*). *Q–T*, calculation of eye pigmentation score. Shown are light microscopic images of the external compound eye of an MJDtr-Q78W fly (*Q*; *MJDw*), the grayscale images extracted from *Q* (*R*), the smoothed image of *R* (*S*), and the binary image of *R* (*T*). *Red outlines* show the region of interest defined to evaluate the eye pigmentation. Note that the images shown here are representative images to explain this procedure clearly. The fly genotype used was *gmr-GAL4/+;;UAS-MJDtr-Q78W/+*. *U* and *V*, quantitative imaging analyses of eye pigmentation in the 1-day-old adult MJDtr-Q78W flies (*U*) or the control 1-day-old adult MJDtr-Q27 flies (*V*) expressing p62-IR alone or bearing *p62* mutations, namely *ref(2)P^{od2}* and *ref(2)P^{od3}*. More than four eye images were analyzed for each genotype. Data are presented as the mean ± S.E. (**, $p < 0.01$; ***, $p < 0.001$; *n.s.*, not significant, *versus* the MJDtr-Q78W flies in *U* and the MJDtr-Q27 flies in *V*, respectively). *W* and *X*, light microscopic images of the external compound eyes of 1-day-old adult flies expressing the Grim protein with or without *p62* knockdown. Fly genotypes were as follows: *gmr-GAL4/+;gmr-grim/+* (*W*) and *gmr-GAL4/+;gmr-grim/UAS-p62-IR* (*X*). *Y*, quantitative imaging analyses of eye pigmentation in the 1-day-old adult *grim* flies with or without expressing p62-IR. More than five eye images were analyzed for each genotype. Data are presented as the mean ± S.E. (*error bars*) (*n.s.*, not significant, *versus* the *grim* flies).

Loss of p62 Function Results in an Increase in Cytoplasmic PolyQ Protein Aggregates—To clarify the mechanisms underlying the protective role of p62 against polyQ protein toxicity, we evaluated the effect of *p62* knockdown on MJDtr-Q78 protein aggregates in the MJDtr-Q78S flies. Immunohistochemical analyses revealed that *p62* knockdown results in a robust increase in MJDtr-Q78 protein aggregates, especially those in the cytoplasm, compared with the control MJDtr-Q78S flies (Fig. 4, *A–D*). Upon quantification of the number of MJDtr-Q78 protein aggregates by imaging analyses (Fig. 4, *E–H*), we found that the increase in the number of MJDtr-Q78 protein aggregates by *p62* knockdown is statistically significant (Fig. 4, *I–K*), but the -fold change in the number of cytoplasmic aggregates was much higher than the -fold change in the number of

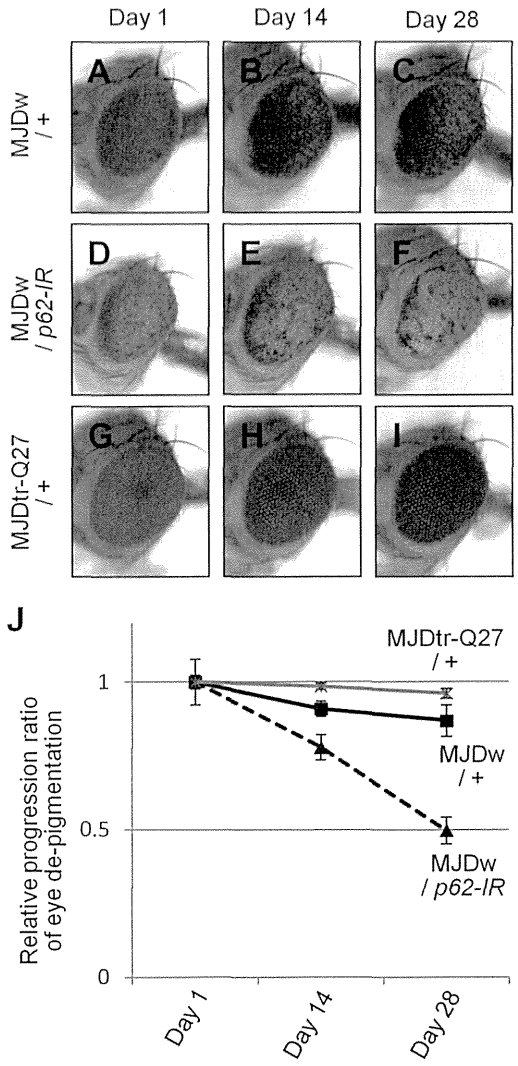

FIGURE 3. **The effect of *p62* knockdown on age-related progression of eye degeneration in the MJDtr-Q78W flies.** *A–F*, light microscopic images of the external compound eyes of 1-, 14-, and 28-day-old adult flies expressing the MJDtr-Q78 protein alone (*A–C*, MJDw/+) or co-expressing p62-IR (*D–F*, MJDw/*p62-IR*) and the control MJDtr-Q27 flies (*G–I*, MJDtr-Q27/+). *J*, relative progression ratio of eye depigmentation by performing quantitative imaging analyses of eye pigmentation in the MJDw flies with or without expressing p62-IR and the MJDtr-Q27 flies, respectively. More than five eye images were analyzed for each genotype. Data are presented as the mean ± S.E. (*error bars*). Fly genotypes were as follows: *gmr-GAL4/+;;UAS-MJDtr-Q78W/+* (*A–C*); *gmr-GAL4/+;UAS-p62-IR/+;UAS-MJDtr-Q78W/+* (*D–F*); and *gmr-GAL4/+;; UAS-MJDtr-Q27/+* (*G–I*).

nuclear aggregates (Fig. 4*L*). These results are consistent with the observation that p62 is predominantly localized in the cytoplasm and co-localizes with cytoplasmic MJDtr-Q78 protein aggregates (Fig. 1). These results suggest that the exacerbation of eye degeneration by *p62* knockdown in the MJDtr-Q78S flies is accompanied by the enhanced accumulation of cytoplasmic MJDtr-Q78 protein aggregates.

Loss of Autophagic Function Causes the Exacerbation of Eye Degeneration Accompanied by the Enhanced Accumulation of Cytoplasmic PolyQ Protein Aggregates—To evaluate whether the intrinsic protein degradation systems are involved in the toxicity of the polyQ protein, we examined the effect of both autophagic deficiency and UPS deficiency in the MJDtr-Q78 flies. For this purpose, we used the RNAi fly lines that express IRs of *Atg12* (autophagy-related gene 12), *alfy* (29), and *Prosβ2* (proteasome β2 subunit) and a mutant fly line of *Atg6* ($Atg6^{00096}$). We found that knockdown of the autophagy-related genes *Atg12* and *alfy* and the *Atg6* mutation result in significant exacerbation of eye degeneration in both the MJDtr-Q78S and MJDtr-Q78W flies (Fig. 5, *A–D*, *F–I*, and *P*). We also found that *Prosβ2* knockdown results in more severe exacerbation of the phenotypes of the MJDtr-Q78 flies, showing a lethal phenotype in the MJDtr-Q78S flies and more severe depigmentation in the MJDtr-Q78W flies (Fig. 5, *E*, *J*, and *P*). We confirmed that knockdown of *Atg12*, *alfy*, or *Prosβ2* or the *Atg6* mutation does not cause any deleterious effects on the eyes of the flies expressing the MJDtr-Q27 protein (Fig. 5, *K–O* and *Q*) or expressing the GAL4 protein alone (data not shown), excluding the possibility that the exacerbation of eye degeneration could be a simple additive effect.

We next evaluated the effects of autophagic or UPS function on MJDtr-Q78 protein aggregates. We found that *Atg12* knockdown significantly increases the number of MJDtr-Q78 protein aggregates, especially those in the cytoplasm, similarly to *p62* knockdown (Fig. 6, *A–D* and *G–J*). In contrast, *Prosβ2* knockdown resulted in a significant increase in MJDtr-Q78 protein aggregates only in the nucleus (Fig. 6, *E–J*). These results are consistent with the fact that protein degradation by autophagy takes place in the cytoplasm. These results imply that p62 plays a role similar to autophagy in the suppression of cytoplasmic polyQ protein aggregate formation.

Protective Role of p62 against PolyQ Protein Toxicity Is Dependent on Autophagy—To clarify whether the effects of *p62* on polyQ protein toxicity are dependent on autophagy or the UPS, we performed genetic analyses to examine the interaction between *p62* and genes involved in these two degradation systems. We crossed MJDtr-Q78W flies co-expressing p62-IR with flies expressing IRs targeted to either autophagy- or UPS-related genes. We found that additional knockdown of either *Atg12* or *alfy* in the MJDtr-Q78W flies together with *p62* knockdown does not show any additive effects on eye degeneration compared with that in the MJDtr-Q78W flies with *p62* knockdown alone (Fig. 7, *A–C* and *I*). On the contrary, additional knockdown of *Prosβ2* resulted in further exacerbation of eye degeneration in the MJDtr-Q78W flies with *p62* knockdown, as confirmed by quantitative imaging analyses (Fig. 7, *D* and *I*). We confirmed that knockdown of *Atg12*, *alfy*, or *Prosβ2* together with *p62* knockdown does not cause any deleterious effects on the eyes of the flies expressing the MJDtr-Q27 protein (Fig. 7, *E–H* and *J*) or expressing the GAL4 protein alone (data not shown), excluding the possibility that the exacerbation of eye degeneration could be a simple additive effect. These results suggest that *p62* plays a protective role against the toxicity of the MJDtr-Q78 protein via autophagy.

Loss of p62 Function Delays the Degradation of the PolyQ Protein in Vivo—To determine the role of p62 in degradation of the polyQ protein, we analyzed the MJDtr-Q78 protein expression level in the MJDtr-Q78S flies with or without *p62* knockdown. Western blot analyses of larval eye disc lysates of the

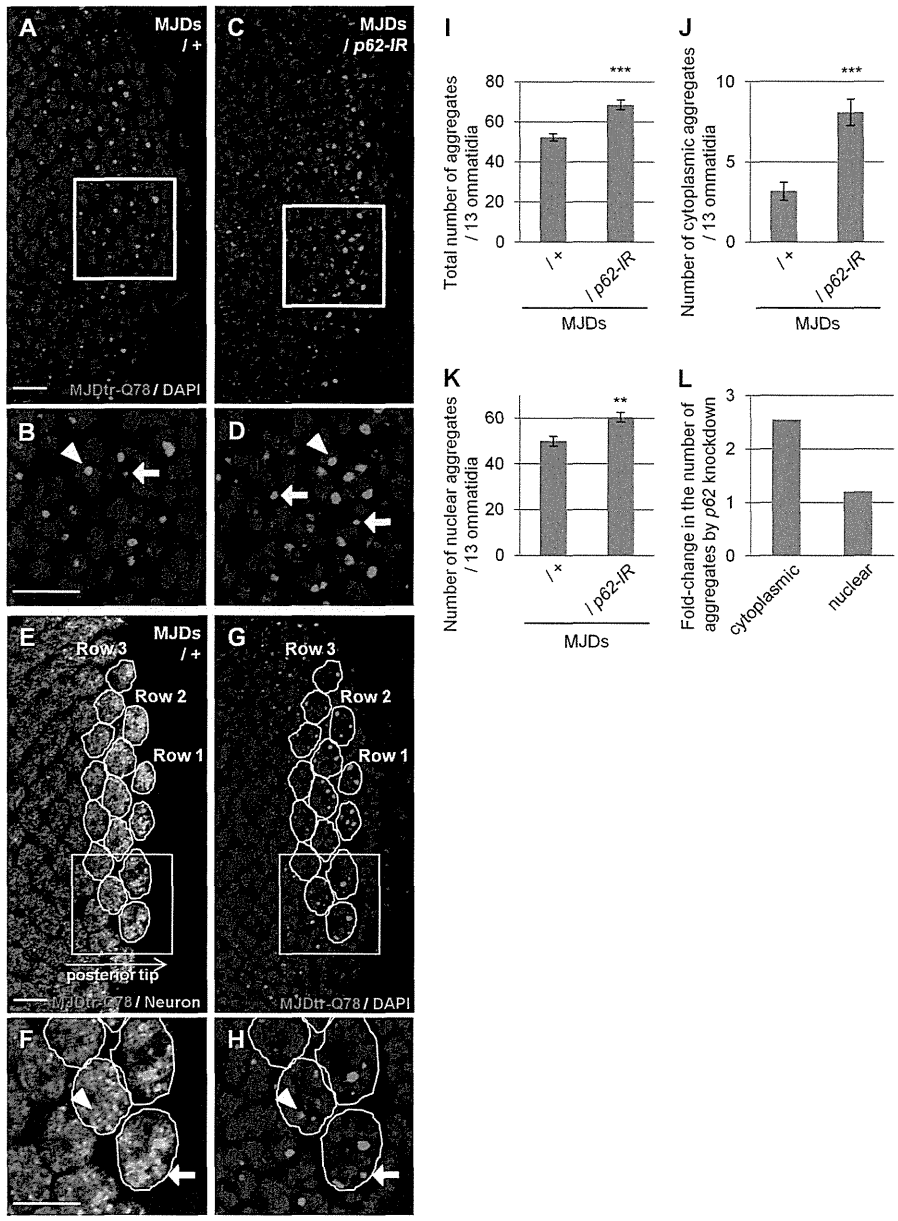

FIGURE 4. **Loss of p62 function results in an increase in cytoplasmic MJDtr-Q78 protein aggregates.** *A–D*, confocal microscopic images of the larval eye discs of flies expressing the MJDtr-Q78 protein alone (*A* and *B*, *MJDs*) or co-expressing p62-IR (*C* and *D*), stained with an anti-HA antibody to detect the MJDtr-Q78 protein (*red*) and DAPI for nuclear staining (*blue*). *B* and *D*, high magnification images of the indicated areas of *A* and *C*, respectively. The *arrows* and *arrowheads* indicate cytoplasmic and nuclear MJDtr-Q78 protein aggregates, respectively. *Bars*, 10 μm. Fly genotypes were as follows: *gmr-GAL4/+;UAS-MJDtr-Q78S/+* (*A* and *B*) and *gmr-GAL4/+;UAS-MJDtr-Q78S/UAS-p62-IR* (*C* and *D*). *E–H*, quantitative analyses of MJDtr-Q78 protein aggregates in the eye discs. Confocal microscopic images of an MJDtr-Q78S fly (MJDs) larval eye disc stained with an anti-HA antibody to detect the MJDtr-Q78 protein (*red*) and with an anti-elav antibody to detect the photoreceptor neurons (*E* and *F*, *green*). Nuclei were stained with DAPI (*G* and *H*, *blue*). Thirteen ommatidia in row 2 and row 3 at the posterior tip of the eye discs were selected (*yellow outlines*). *F* and *H*, high magnification images of the indicated areas of *E* and *G*, respectively. The MJDtr-Q78 protein aggregates were counted as either cytoplasmic aggregates (*arrow*) or nuclear aggregates (*arrowhead*), depending on whether they merged with the nucleus or not. The fly genotype used was *gmr-GAL4/+;UAS-MJDtr-Q78S/+*. *Bars*, 10 μm. *I–K*, the number of MJDtr-Q78 protein aggregates in the eye discs of MJDtr-Q78S flies with or without expression of p62-IR. The total numbers of MJDtr-Q78 protein aggregates (*I*), cytoplasmic aggregates (*J*), and nuclear aggregates (*K*) are presented. More than five eye discs were analyzed for both genotypes. Data are presented as the mean ± S.E. (*error bars*) (**, $p < 0.01$; ***, $p < 0.001$, *versus* the MJDtr-Q78S flies). *L*, the -fold change in the number of cytoplasmic or nuclear MJDtr-Q78 protein aggregates by *p62* knockdown.

MJDtr-Q78S flies constitutively expressing the MJDtr-Q78 protein by the *gmr-GAL4* driver revealed that knockdown of neither *p62* nor *Atg12* affects the MJDtr-Q78 protein expression level (Fig. 8, *A* and *B*). Because the MJDtr-Q78 protein expression level is dependent on the equilibrium between its expression and degradation, constitutive expression of the MJDtr-Q78 protein by the *gmr-GAL4* driver may make it difficult to detect alterations in MJDtr-Q78 protein turnover. Therefore, to evaluate MJDtr-Q78 protein turnover, we next used the inducible MJDtr-Q78S fly line, namely "ind-MJDtr-

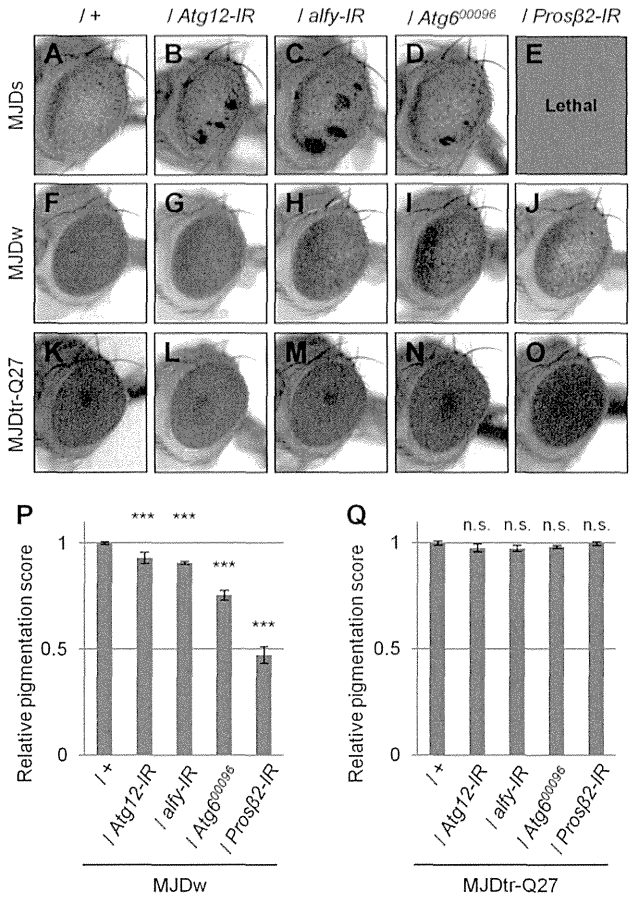

FIGURE 5. **Loss of autophagic or proteasomal function causes exacerbation of eye degeneration in MJDtr-Q78 flies.** *A–O*, light microscopic images of the external compound eyes of 1-day-old adult flies of two different MJDtr-Q78 fly lines, MJDtr-Q78S flies (*A*, *MJDs*) and MJDtr-Q78W flies (*F*, *MJDw*); MJDtr-Q78 flies co-expressing Atg12-IR (*B* and *G*), alfy-IR (*C* and *H*), or the proteasome β2 subunit (Prosβ2)-IR (*E* and *J*) or bearing an *Atg6* mutation (*Atg6*^{00096}) (*D* and *I*); and the control 1-day-old adult MJDtr-Q27 flies (*K–O*). Note that *Prosβ2* knockdown showed a lethal phenotype in the MJDtr-Q78S flies. Fly genotypes were as follows: *gmr-GAL4/+;UAS-MJDtr-Q78S/+* (*A*); *gmr-GAL4/+;UAS-MJDtr-Q78S/UAS-Atg12-IR* (*B*); *gmr-GAL4/+;UAS-MJDtr-Q78S/alfy-IR* (*C*); *gmr-GAL4/+;UAS-MJDtr-Q78S/+;Atg6*^{00096}*/+* (*D*); *gmr-GAL4/+;UAS-MJDtr-Q78S/+;Prosβ2-IR/+* (*E*); *gmr-GAL4/+;;UAS-MJDtr-Q78W/+* (*F*); *gmr-GAL4/+;UAS-Atg12-IR/+;UAS-MJDtr-Q78W/+* (*G*); *gmr-GAL4/+;UAS-alfy-IR/+;UAS-MJDtr-Q78W/+* (*H*); *gmr-GAL4/+;;UAS-MJDtr-Q78W/Atg6*^{00096} (*I*); *gmr-GAL4/+;;UAS-MJDtr-Q78W/Prosβ2-IR* (*J*); *gmr-GAL4/+;;UAS-MJDtr-Q27/+* (*K*); *gmr-GAL4/+;UAS-Atg12-IR/+;UAS-MJDtr-Q27/+* (*L*); *gmr-GAL4/+; alfy-IR/+;UAS-MJDtr-Q27/+* (*M*); *gmr-GAL4/+;;UAS-MJDtr-Q27/Atg6*^{00096} (*N*); and *gmr-GAL4/+;;UAS-MJDtr-Q27/Prosβ2-IR* (*O*). *P* and *Q*, quantitative imaging analyses of eye pigmentation in the 1-day-old adult MJDtr-Q78W flies (*P*) or the control 1-day-old adult MJDtr-Q27 flies (*Q*) expressing Atg12-IR, alfy-IR, or Prosβ2-IR or bearing an *Atg6* mutation. More than four eye images were analyzed for each genotype. Data are presented as the mean ± S.E. (*error bars*) (***, $p < 0.001$; *n.s.*, not significant, *versus* the MJDtr-Q78W flies in *P* and *versus* the MJDtr-Q27 flies in *Q*, respectively).

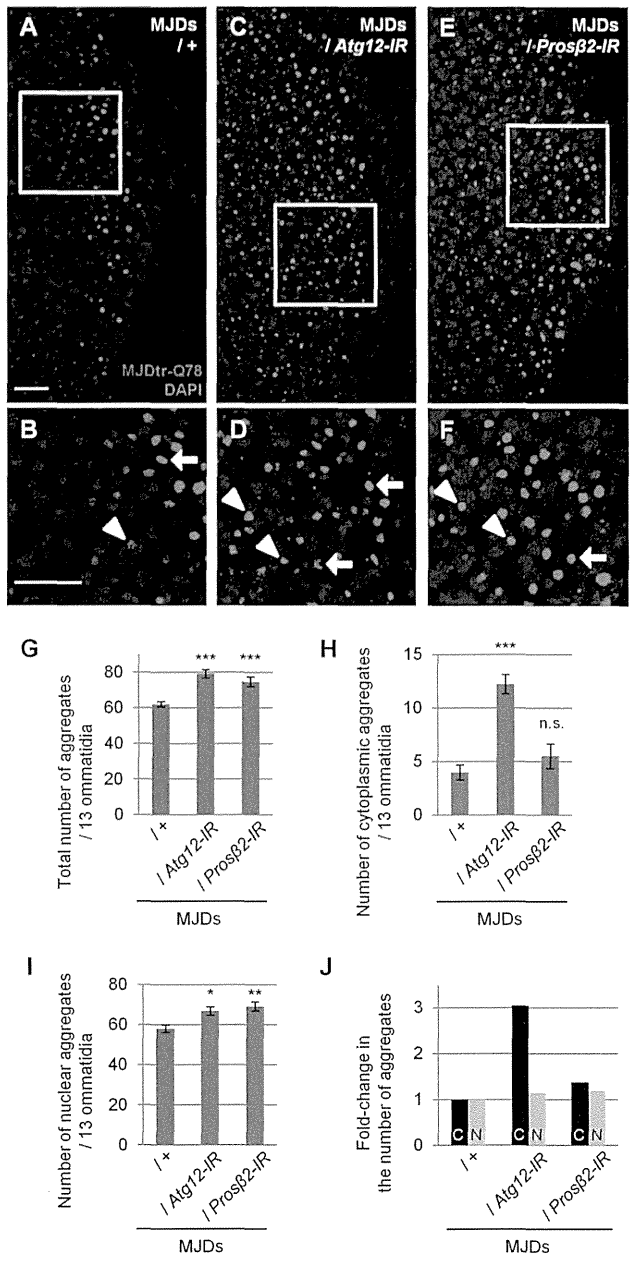

FIGURE 6. **Loss of autophagic function results in an increase in cytoplasmic MJDtr-Q78 protein aggregates.** *A–F*, confocal microscopic images of larval eye discs of flies expressing the MJDtr-Q78S protein alone (*A* and *B*, *MJDs*) or co-expressing either Atg12-IR (*C* and *D*) or the proteasome β2 subunit (*Prosβ2*)-IR (*E* and *F*), stained with an anti-HA antibody to detect the MJDtr-Q78 protein (*red*) and DAPI for nuclear staining (*blue*). *B*, *D*, and *F*, high magnification images of the indicated areas of *A*, *C*, and *E*, respectively. The *arrows* and *arrowheads* indicate cytoplasmic and nuclear MJDtr-Q78 protein aggregates, respectively. *Bars*, 10 μm. Fly genotypes used were as follows: *gmr-GAL4/+;UAS-MJDtr-Q78S/+* (*A* and *B*); *gmr-GAL4/+;UAS-MJDtr-Q78S/UAS-Atg12-IR* (*C* and *D*); and *gmr-GAL4/+;UAS-MJDtr-Q78S/+;Prosβ2-IR/+* (*E* and *F*). *G–I*, number of MJDtr-Q78 protein aggregates in the eye discs of MJDtr-Q78S flies with or without expression of Atg12-IR or Prosβ2-IR. The total numbers of MJDtr-Q78 protein aggregates (*G*), cytoplasmic aggregates (*H*), and nuclear aggregates (*I*) are presented. More than five eye discs were analyzed for each genotype. Data are presented as the mean ± S.E. (*error bars*) (*, $p < 0.05$; **, < 0.01; ***, $p < 0.001$; *n.s.*, not significant, *versus* the MJDtr-Q78S flies). *J*, -fold change in the number of cytoplasmic (*C*) or nuclear (*N*) MJDtr-Q78 protein aggregates by knockdown of *Atg12* or *Prosβ2*.

Q78S," which expresses the MJDtr-Q78 protein only in the presence of RU486 (mifepristone) under the control of the *gmr*-GeneSwitch (*gmr-GS*) driver (30). To validate this drug-inducible system *in vivo*, we evaluated the decay of the MJDtr-Q78 protein by Western blot analysis. RU486 was administered orally to ind-MJDtr-Q78 flies during the larval stage to induce MJDtr-Q78 protein expression. After emergence, RU486 was withdrawn to abolish MJDtr-Q78 protein expression. Western

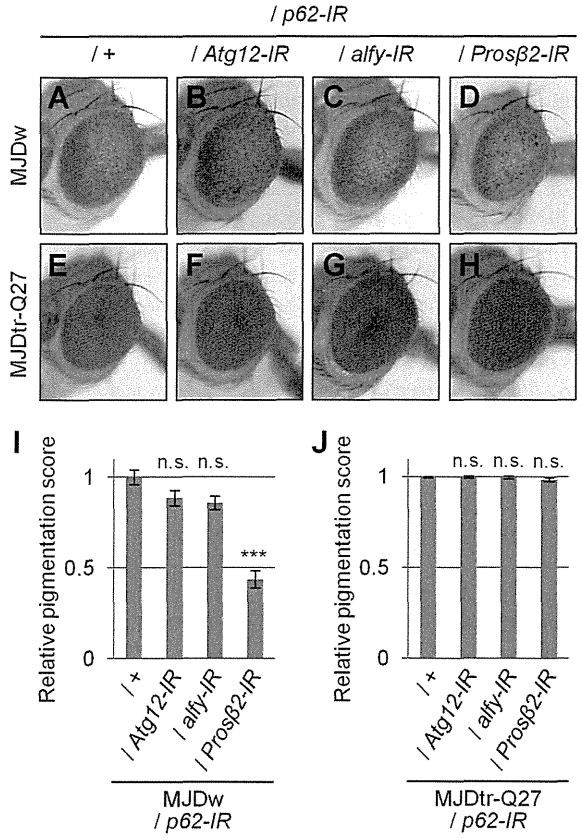

FIGURE 7. **Knockdown of autophagy-related genes in addition to *p62* knockdown does not cause additive exacerbation of eye degeneration in MJDtr-Q78W flies.** *A–H*, light microscopic images of the external compound eyes of 1-day-old adult MJDtr-Q78W (*MJDw*) flies with *p62* knockdown alone (*A*) or together with *Atg12* knockdown (*B*), *alfy* knockdown (*C*), or knockdown of *Prosβ2* (*D*) and the control 1-day-old adult MJDtr-Q27 flies (*E–H*). Fly genotypes used were as follows: *gmr-GAL4/+;UAS-p62-IR/+;UAS-MJDtr-Q78W/+* (*A*); *gmr-GAL4/+;UAS-p62-IR/UAS-Atg12-IR/+;UAS-MJDtr-Q78W/+* (*B*) *gmr-GAL4/+;UAS-p62-IR/UAS-alfy-IR;UAS-MJDtr-Q78W/+* (*C*); *gmr-GAL4/+;UAS-p62-IR/+;UAS-MJDtr-Q78W/Prosβ2-IR* (*D*); *gmr-GAL4/+;UAS-p62-IR/+;UAS-MJDtr-Q27/+* (*E*); *gmr-GAL4/+;UAS-p62-IR/UAS-Atg12-IR;UAS-MJDtr-Q27/+* (*F*); *gmr-GAL4/+;UAS-p62-IR/alfy-IR;UAS-MJDtr-Q27/+* (*G*); and *gmr-GAL4/+;UAS-p62-IR/+;UAS-MJDtr-Q27/Prosβ2-IR* (*H*). *I* and *J*, quantitative imaging analyses of eye pigmentation in the 1-day-old adult MJDtr-Q78W flies (*I*) or the control 1-day-old adult MJDtr-Q27 flies (*J*) with *p62* knockdown alone or together with *Atg12* knockdown, *alfy* knockdown, or *Prosβ2* knockdown. More than five eye images were analyzed for each genotype. Data are presented as the mean ± S.E. (*error bars*) (***, $p < 0.001$; *n.s.*, not significant, *versus* the MJDtr-Q78W flies with *p62* knockdown in *I* and *versus* the MJDtr-Q27 flies in *J*, respectively).

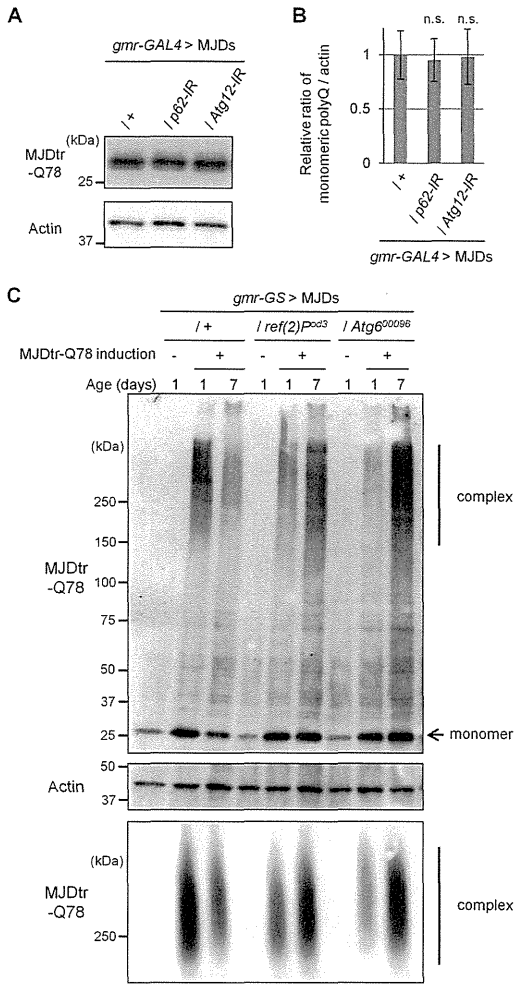

FIGURE 8. **Loss of p62 function delays the degradation of the MJDtr-Q78 protein *in vivo*.** *A* and *B*, Western blot analysis of the monomeric MJDtr-Q78 protein in larval eye disc lysates of the MJDtr-Q78S flies (*MJDs*) expressing the MJDtr-Q78 protein alone (+) or co-expressing either p62-IR or Atg12-IR under the *gmr-GAL4* driver, using an anti-HA antibody to detect the MJDtr-Q78 protein. The expression level of actin was used as a protein-loading control. The graph shows the ratio of the MJDtr-Q78 protein to actin. The relative amount of each protein was measured by densitometric analysis of the bands in *A*. Data are presented as the mean ± S.E. (*error bars*) (*n.s.*, not significant, *versus* the MJDtr-Q78S flies) ($n = 3–4$). Fly genotypes used were *gmr-GAL4/+;UAS-MJDtr-Q78S/+*, *gmr-GAL4/+;UAS-MJDtr-Q78S/UAS-p62-IR*, and *gmr-GAL4/+;UAS-MJDtr-Q78S/UAS-Atg12-IR*. *C*, Western blot analysis (*top* and *middle panels*) and SDS-AGE (*bottom panel*) of the MJDtr-Q78 protein in lysates prepared from 1-day-old and 7-day-old adult fly heads, expressing the MJDtr-Q78 protein alone (+) or bearing either the *p62* mutation (*ref(2)P*^{od3}) or *Atg6* mutation (*Atg6*^{00096}), under the *gmr*-GeneSwitch (*gmr-GS*) driver. MJDtr-Q78 protein expression was induced only during the larval stage by RU486 treatment (10 μg/ml) for the evaluation of MJDtr-Q78 protein turnover. In Western blot analysis, the monomeric MJDtr-Q78 protein (*monomer*) and its high molecular weight complexes (*complex*) were detected with an anti-HA antibody. The expression level of actin was used as a protein-loading control. The groups without MJDtr-Q78 protein induction (−) were evaluated for leak MJDtr-Q78 protein expression. In SDS-AGE, the high molecular weight complexes of the MJDtr-Q78 protein were detected with an anti-HA antibody. Fly genotypes used were *gmr-GS/+;UAS-MJDtr-Q78S/+*, *gmr-GS/+;UAS-MJDtr-Q78S/ref(2)P*^{od3}, and *gmr-GS/+;UAS-MJDtr-Q78S/+;Atg6*^{00096}*/+*.

blot analyses of lysates prepared from these adult fly heads demonstrated the gradual reduction of MJDtr-Q78 protein levels in the 7-day-old flies compared with the 1-day-old flies (Fig. 8*C*, +). These results suggest that both the monomeric MJDtr-Q78 protein and its high molecular weight complexes are efficiently degraded during the 6 days after emergence. The ind-MJDtr-Q78S flies without RU486 treatment showed slight leak expression of the MJDtr-Q78 protein. In this condition, we next analyzed the effects of p62 or autophagic deficiency on MJDtr-Q78 protein turnover. We crossed the ind-MJDtr-Q78S flies with *p62* or *Atg6* mutant flies, which are deficient in their functions independent of RU486 treatment. Western blot analyses showed that loss of p62 function clearly delays the degradation of both monomeric and high molecular weight complexes of the MJDtr-Q78 protein, similarly to loss of Atg6 function (Fig. 8*C*, *top* and *middle panels*). Surprisingly, the amounts of high molecular weight complexes of the MJDtr-Q78 protein were

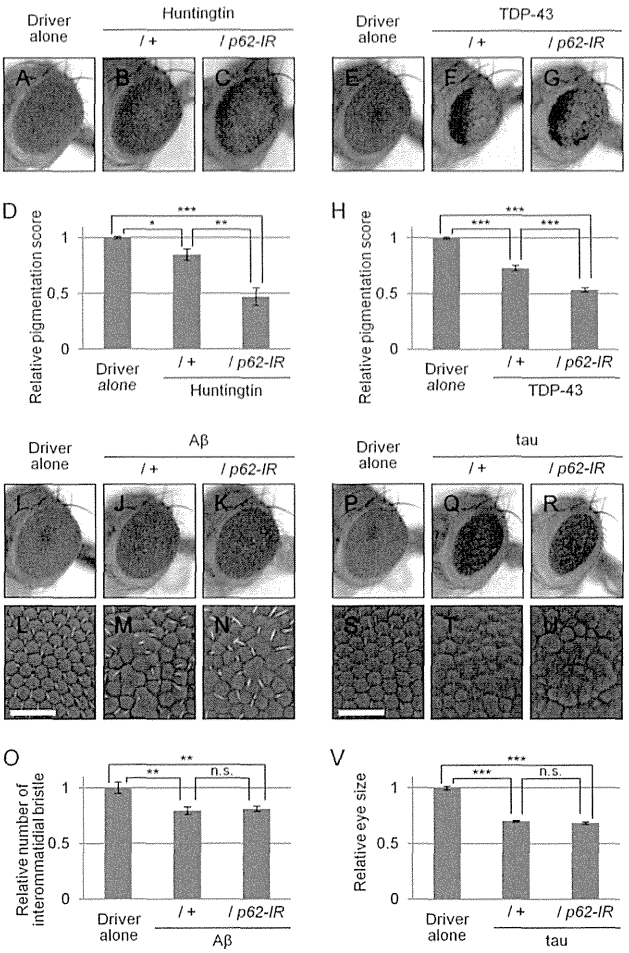

FIGURE 9. **Effects of loss of p62 function in various neurodegenerative disease model flies.** *A–C*, light microscopic images of the external compound eyes of 1-day-old adult flies expressing the mutant huntingtin protein with an expanded Gln-97 repeat with or without *p62* knockdown (*B* and *C*) and the control flies expressing the GAL4 protein alone (*A*). Fly genotypes used were as follows: *gmr-GAL4/+* (*A*); *gmr-GAL4/+;;UAS-Httex1p97QP/+* (*B*); *gmr-GAL4/+;UAS-p62-IR/+;UAS-Httex1p97QP/+* (*C*). *D*, quantitative imaging analyses of eye pigmentation in *A–C*. More than five eye images were analyzed for each genotype. Data are presented as the mean ± S.E. (*error bars*) (*, $p < 0.05$; **, $p < 0.01$; ***, $p < 0.001$, *versus* the control flies expressing the GAL4 protein alone). *E–G*, light microscopic images of the external compound eyes of 7-day-old adult flies expressing the human TDP-43 protein with or without *p62* knockdown (*F* and *G*), and the control flies expressing the GAL4 protein alone (*E*). Fly genotypes used were as follows: *gmr-GAL4/+* (*E*); *gmr-GAL4/+;UAS-*human *TDP-43/+* (*F*); and *gmr-GAL4/+;UAS-human TDP-43/UAS-p62-IR* (*G*). *H*, quantitative imaging analyses of eye pigmentation in *E–G*. More than five eye images were analyzed for each genotype. Data are presented as the mean ± S.E. (***, $p < 0.001$, *versus* the control flies expressing the GAL4 protein alone). *I–N*, light microscopic images (*I–K*) and SEM images (*L–N*) of the external compound eyes of 1-day-old adult flies expressing the mutant Aβ protein with or without *p62* knockdown (*J*, *K*, *M*, and *N*) and the control flies expressing the GAL4 protein alone (*I* and *L*). *Bars*, 50 μm. Fly genotypes used were as follows: *gmr-GAL4/+* (*I* and *L*); *gmr-GAL4/+;;UAS-Aβ arc2* (*J* and *M*); and *gmr-GAL4/+;UAS-p62-IR/+;UAS-Aβ arc2/+* (*K* and *N*). *O*, quantitative imaging analyses of the number of the interommatidial bristles in *L–N*. More than seven eye images were analyzed for each genotype. Data are presented as the mean ± S.E. (**, $p < 0.01$; n.s., not significant, *versus* the control flies expressing the GAL4 protein alone). *P–U*, light microscopic images (*P–R*) and SEM images (*S–U*) of the external compound eyes of 1-day-old adult flies expressing the mutant Tau protein with or without *p62* knockdown (*Q*, *R*, *T*, and *U*) and the control flies expressing the GAL4 protein alone (*P* and *S*). *Bars*, 50 μm. Fly genotypes used were as follows: *gmr-GAL4/+* (*P* and *S*); *gmr-GAL4/+;;UAS-R406W tau/+* (*Q* and *T*); and *gmr-GAL4/+;UAS-p62-IR/+; UAS-R406W tau/+* (*R* and *U*). *V*, quantitative imaging analyses of the eye size in *P–R*. More than 10 eye images were analyzed for each genotype. Data are presented as the mean ± S.E. (***, $p < 0.001$; *n.s.*, not significant, *versus* the control flies expressing the GAL4 protein alone).

rather increased by the loss of p62 or Atg6 function in the 7-day-old flies, implying that the monomeric MJDtr-Q78 protein that escaped from degradation assembles into oligomers during the 6 days. To further characterize these high molecular weight complexes of the MJDtr-Q78 protein, we performed the SDS-AGE blotting, allowing for the detection of SDS-soluble oligomeric species (25–27). The amounts of the slowly migrating SDS-soluble oligomeric species of the MJDtr-Q78 protein were clearly increased by the loss of p62 or Atg6 function in the 7-day-old flies, consistent with the results of Western blot analyses (Fig. 8*C*, *bottom panel*). These results suggest that loss of p62 function impairs autophagic degradation of the MJDtr-Q78 protein, especially its oligomeric species.

p62 Plays a Protective Role in Various Neurodegenerative Disease Model Flies—To evaluate whether the protective role of p62 is specific to MJDtr-Q78 flies, we examined the effects of *p62* knockdown in various neurodegenerative disease model flies. We used the Huntington disease model flies expressing a mutant huntingtin protein with an expanded Gln-97 repeat (19), the Alzheimer disease model flies expressing the mutant amyloid-β (Aβ) protein (20), the ALS model flies expressing the human TDP-43 protein, and the tauopathy model flies expressing the mutant Tau protein (21). In the huntingtin flies, *p62* knockdown resulted in significant exacerbation of eye degeneration, similarly to the MJDtr-Q78 flies (Fig. 9, *A–C*). Upon quantification of the eye pigmentation by imaging analyses in this model flies, the exacerbation of eye depigmentation by *p62* knockdown was statistically significant (Fig. 9*D*). In the TDP-43 flies, *p62* knockdown also resulted in significant exacerbation of eye degeneration (Fig. 9, *E–G*). Upon quantification of the eye pigmentation by imaging analyses in flies of this model, the exacerbation of eye depigmentation by *p62* knockdown was also statistically significant (Fig. 9*H*). On the contrary, the Aβ flies and the Tau flies did not show exacerbation of eye degeneration by *p62* knockdown, as revealed by both light microscopic and SEM analyses, respectively (Fig. 9, *I–N* and *P–U*). Upon quantification of the number of interommatidial bristles in the Aβ flies (Fig. 9, *L–N*) or the eye size in the Tau flies (Fig. 9, *P–R*), the exacerbation of eye degeneration by *p62* knockdown in both flies was not statistically significant (Fig. 9, *O* and *V*). These results suggest that p62 exerts protective effects not only against the polyQ protein but also against other proteins associated with neurodegenerative diseases.

DISCUSSION

In the present study, we provide evidence that p62 plays a protective role in the polyQ diseases *in vivo*. We demonstrated that the loss of p62 function causes a delay in the autophagic degradation of the polyQ protein, resulting in the enhanced accumulation of polyQ protein oligomers and cytoplasmic aggregates, and eventually leads to the exacerbation of the eye degeneration of polyQ disease model flies. We also genetically showed that these functions of p62 are dependent on autophagy. These results suggest that degradation of polyQ

protein oligomers is one of the important roles of p62 in protecting against polyQ protein toxicity.

Because p62 is delivered to the autophagosome by interaction with autophagosome membrane light chain 3 via the light chain 3-interacting region of p62 and recognizes ubiquitinated proteins via the ubiquitin-associated domain, p62 was suggested to be engaged in the selective autophagic degradation of ubiquitinated proteins, including the polyQ protein (13, 14). However, there have been substantial controversies regarding the role of p62 in polyQ cell culture models; one study reported that p62 depletion accelerates polyQ-induced cytotoxicity and it is rescued by p62 overexpression (28), whereas another study reported that p62 overexpression accelerates polyQ-induced cytotoxicity (31). In addition, some studies reported that p62 depletion does not affect the formation of polyQ protein aggregates (31–33). In this study, using polyQ disease model flies, we demonstrated that p62 depletion delays the autophagic degradation of the polyQ protein, including its oligomeric species, not merely its monomer. Our results are consistent with a recent report that depletion of p62 induces the accumulation of polyQ proteins in spinobulbar muscular atrophy model mice (34). These results suggest that p62-mediated autophagic degradation of the polyQ protein contributes to the protective effects of p62 against polyQ protein toxicity.

Our study clearly indicates the tight correlation between the amount of polyQ protein oligomers and the degree of neurodegeneration upon the loss of p62 function. Although several studies reported that the amount of polyQ protein inclusions does not correlate with neurodegeneration or that these inclusions are even protective, oligomeric species of misfolded polyQ proteins have been suggested as the principal culprit of neurodegeneration (6, 35). In other protein-misfolding neurodegenerative diseases, soluble oligomers composed of Aβ or α-synuclein have also been shown to exert cytotoxicity, suggesting the intrinsic toxicity of oligomeric structures, regardless of their primary amino acid sequences (36).

Although autophagy is known to act in the cytoplasm, our immunohistochemical analyses showed that p62 depletion also results in a modest increase in nuclear polyQ protein aggregates (Figs. 4 and 6). These results may be a secondary consequence of inefficient autophagic degradation of the polyQ protein, because Atg12 depletion also resulted in a similar consequence. A possible explanation for these results is that inefficient degradation of the polyQ protein in the cytoplasm may also result in an increase of polyQ proteins in the nucleus and their accumulation as nuclear aggregates.

In this study, we showed the protective role of p62 not only in the MJDtr-Q78 flies but also in other neurodegenerative disease flies, such as Huntington disease and TDP-43 proteinopathies (Fig. 9). These results are consistent with the previous reports that huntingtin and TDP-43 are degraded by autophagy (37–40). However, we could not detect the protective effect of p62 in the Aβ flies and the Tau flies. It is known that these Tau-expressing flies do not develop tangles consisting of misfolded Tau proteins (21). Moreover, the Tau protein is reported to be mainly degraded by the UPS rather than autophagy (41–43). In addition, the Aβ peptides are not ubiquitinated in the Alzheimer disease brain, and they are known to be degraded by endopeptidases, such as neprilysin and insulin-degrading enzyme (44, 45). Therefore, p62 could be involved in neurodegeneration in the polyQ and TDP-43 flies but not in the Aβ and Tau flies, although further studies are required to elucidate the mechanisms of the selectivity of p62.

Our study provides new evidence that p62 is involved in the autophagic degradation of the polyQ protein, including its oligomers, *in vivo*, indicating its therapeutic potential for the polyQ diseases. Considering the selectivity of p62 for ubiquitinated proteins, the next step toward developing a p62-based therapy for the polyQ diseases should be establishing a method for the efficient recognition and degradation of polyQ proteins and possibly other misfolded proteins. A recent study revealed that phosphorylation of p62 at serine 403 renders a higher affinity to the polyubiquitin chain, resulting in the efficient degradation of ubiquitinated proteins (33). Selective and efficient degradation of misfolded proteins, especially oligomers, by p62 is expected to be developed as a general therapeutic strategy against protein-misfolding neurodegenerative diseases in the future.

Acknowledgments—We thank Drs. E. N. Minakawa (National Center of Neurology and Psychiatry), T. Takeuchi (Kyoto University), M. Komatsu (Niigata University), and T. Yoshimori (Osaka University) for helpful discussions; Dr. D. Contamine (deceased; Université Versailles-St Quentin-en-Yvelines) for kindly providing the mutant fly lines ref(2)P^{od2} and ref(2)P^{od3} and the rabbit polyclonal anti-Ref(2)P/p62 antibody; and the Bloomington Drosophila Stock Center and the Vienna Drosophila Resource Center for the other fly lines. We also thank T. Okada for technical assistance.

REFERENCES

1. Gatchel, J. R., and Zoghbi, H. Y. (2005) Diseases of unstable repeat expansion: mechanisms and common principles. *Nat. Rev. Genet.* **6,** 743–755
2. Davies, S. W., Turmaine, M., Cozens, B. A., DiFiglia, M., Sharp, A. H., Ross, C. A., Scherzinger, E., Wanker, E. E., Mangiarini, L., and Bates, G. P. (1997) Formation of neuronal intranuclear inclusions underlies the neurological dysfunction in mice transgenic for the HD mutation. *Cell* **90,** 537–548
3. Scherzinger, E., Lurz, R., Turmaine, M., Mangiarini, L., Hollenbach, B., Hasenbank, R., Bates, G. P., Davies, S. W., Lehrach, H., and Wanker, E. E. (1997) Huntingtin-encoded polyglutamine expansions form amyloid-like protein aggregates *in vitro* and *in vivo*. *Cell* **90,** 549–558
4. Arrasate, M., Mitra, S., Schweitzer, E. S., Segal, M. R., and Finkbeiner, S. (2004) Inclusion body formation reduces levels of mutant huntingtin and the risk of neuronal death. *Nature* **431,** 805–810
5. Nagai, Y., Inui, T., Popiel, H. A., Fujikake, N., Hasegawa, K., Urade, Y., Goto, Y., Naiki, H., and Toda, T. (2007) A toxic monomeric conformer of the polyglutamine protein. *Nat. Struct. Mol. Biol.* **14,** 332–340
6. Takahashi, T., Kikuchi, S., Katada, S., Nagai, Y., Nishizawa, M., and Onodera, O. (2008) Soluble polyglutamine oligomers formed prior to inclusion body formation are cytotoxic. *Hum. Mol. Genet.* **17,** 345–356
7. Rubinsztein, D. C. (2006) The roles of intracellular protein-degradation pathways in neurodegeneration. *Nature* **443,** 780–786
8. Verhoef, L. G., Lindsten, K., Masucci, M. G., and Dantuma, N. P. (2002) Aggregate formation inhibits proteasomal degradation of polyglutamine proteins. *Hum. Mol. Genet.* **11,** 2689–2700
9. Holmberg, C. I., Staniszewski, K. E., Mensah, K. N., Matouschek, A., and Morimoto, R. I. (2004) Inefficient degradation of truncated polyglutamine proteins by the proteasome. *EMBO J.* **23,** 4307–4318
10. Venkatraman, P., Wetzel, R., Tanaka, M., Nukina, N., and Goldberg, A. L. (2004) Eukaryotic proteasomes cannot digest polyglutamine sequences and release them during degradation of polyglutamine-containing proteins. *Mol. Cell* **14,** 95–104

11. Ravikumar, B., Duden, R., and Rubinsztein, D. C. (2002) Aggregate-prone proteins with polyglutamine and polyalanine expansions are degraded by autophagy. *Hum. Mol. Genet.* **11,** 1107–1117
12. Johansen, T., and Lamark, T. (2011) Selective autophagy mediated by autophagic adapter proteins. *Autophagy* **7,** 279–296
13. Pankiv, S., Clausen, T. H., Lamark, T., Brech, A., Bruun, J. A., Outzen, H., Øvervatn, A., Bjørkøy, G., and Johansen, T. (2007) p62/SQSTM1 binds directly to Atg8/LC3 to facilitate degradation of ubiquitinated protein aggregates by autophagy. *J. Biol. Chem.* **282,** 24131–24145
14. Ichimura, Y., Kumanomidou, T., Sou, Y. S., Mizushima, T., Ezaki, J., Ueno, T., Kominami, E., Yamane, T., Tanaka, K., and Komatsu, M. (2008) Structural basis for sorting mechanism of p62 in selective autophagy. *J. Biol. Chem.* **283,** 22847–22857
15. Kuusisto, E., Salminen, A., and Alafuzoff, I. (2001) Ubiquitin-binding protein p62 is present in neuronal and glial inclusions in human tauopathies and synucleinopathies. *Neuroreport* **12,** 2085–2090
16. Kuusisto, E., Kauppinen, T., and Alafuzoff, I. (2008) Use of p62/SQSTM1 antibodies for neuropathological diagnosis. *Neuropathol. Appl. Neurobiol.* **34,** 169–180
17. Yamaguchi, M., Hirose, F., Inoue, Y. H., Shiraki, M., Hayashi, Y., Nishi, Y., and Matsukage, A. (1999) Ectopic expression of human p53 inhibits entry into S phase and induces apoptosis in the *Drosophila* eye imaginal disc. *Oncogene* **18,** 6767–6775
18. Warrick, J. M., Paulson, H. L., Gray-Board, G. L., Bui, Q. T., Fischbeck, K. H., Pittman, R. N., and Bonini, N. M. (1998) Expanded polyglutamine protein forms nuclear inclusions and causes neural degeneration in *Drosophila*. *Cell* **93,** 939–949
19. Steffan, J. S., Agrawal, N., Pallos, J., Rockabrand, E., Trotman, L. C., Slepko, N., Illes, K., Lukacsovich, T., Zhu, Y. Z., Cattaneo, E., Pandolfi, P. P., Thompson, L. M., and Marsh, J. L. (2004) SUMO modification of Huntingtin and Huntington's disease pathology. *Science* **304,** 100–104
20. Crowther, D. C., Kinghorn, K. J., Miranda, E., Page, R., Curry, J. A., Duthie, F. A., Gubb, D. C., and Lomas, D. A. (2005) Intraneuronal Aβ, non-amyloid aggregates and neurodegeneration in a *Drosophila* model of Alzheimer's disease. *Neuroscience* **132,** 123–135
21. Wittmann, C. W., Wszolek, M. F., Shulman, J. M., Salvaterra, P. M., Lewis, J., Hutton, M., and Feany, M. B. (2001) Tauopathy in *Drosophila*: neurodegeneration without neurofibrillary tangles. *Science* **293,** 711–714
22. Wyers, F., Petitjean, A. M., Dru, P., Gay, P., and Contamine, D. (1995) Localization of domains within the *Drosophila* Ref(2)P protein involved in the intracellular control of σ rhabdovirus multiplication. *J. Virol.* **69,** 4463–4470
23. Ueyama, M., Takemae, H., Ohmae, Y., Yoshida, H., Toyoda, H., Ueda, R., and Nishihara, S. (2008) Functional analysis of proteoglycan galactosyltransferase II RNA interference mutant flies. *J. Biol. Chem.* **283,** 6076–6084
24. Menzies, F. M., Garcia-Arencibia, M., Imarisio, S., O'Sullivan, N. C., Ricketts, T., Kent, B. A., Rao, M. V., Lam, W., Green-Thompson, Z. W., Nixon, R. A., Saksida, L. M., Bussey, T. J., O'Kane, C. J., and Rubinsztein, D. C. (2014) Calpain inhibition mediates autophagy-dependent protection against polyglutamine toxicity. *Cell Death Differ.* 10.1038/cdd.2014.151
25. Weiss, A., Klein, C., Woodman, B., Sathasivam, K., Bibel, M., Régulier, E., Bates, G. P., and Paganetti, P. (2008) Sensitive biochemical aggregate detection reveals aggregation onset before symptom development in cellular and murine models of Huntington's disease. *J. Neurochem.* **104,** 846–858
26. Legleiter, J., Mitchell, E., Lotz, G. P., Sapp, E., Ng, C., DiFiglia, M., Thompson, L. M., and Muchowski, P. J. (2010) Mutant huntingtin fragments form oligomers in a polyglutamine length-dependent manner *in vitro* and *in vivo*. *J. Biol. Chem.* **285,** 14777–14790
27. Sontag, E. M., Lotz, G. P., Yang, G., Sontag, C. J., Cummings, B. J., Glabe, C. G., Muchowski, P. J., and Thompson, L. M. (2012) Detection of mutant huntingtin aggregation conformers and modulation of SDS-soluble fibrillar oligomers by small molecules. *J. Huntingtons Dis.* **1,** 127–140
28. Bjørkøy, G., Lamark, T., Brech, A., Outzen, H., Perander, M., Overvatn, A., Stenmark, H., and Johansen, T. (2005) p62/SQSTM1 forms protein aggregates degraded by autophagy and has a protective effect on huntingtin-induced cell death. *J. Cell Biol.* **171,** 603–614
29. Filimonenko, M., Isakson, P., Finley, K. D., Anderson, M., Jeong, H., Melia, T. J., Bartlett, B. J., Myers, K. M., Birkeland, H. C., Lamark, T., Krainc, D., Brech, A., Stenmark, H., Simonsen, A., and Yamamoto, A. (2010) The selective macroautophagic degradation of aggregated proteins requires the PI3P-binding protein Alfy. *Mol. Cell* **38,** 265–279
30. Roman, G., and Davis, R. L. (2002) Conditional expression of UAS-transgenes in the adult eye with a new gene-switch vector system. *Genesis* **34,** 127–131
31. Korolchuk, V. I., Mansilla, A., Menzies, F. M., and Rubinsztein, D. C. (2009) Autophagy inhibition compromises degradation of ubiquitin-proteasome pathway substrates. *Mol. Cell* **33,** 517–527
32. Nagaoka, U., Kim, K., Jana, N. R., Doi, H., Maruyama, M., Mitsui, K., Oyama, F., and Nukina, N. (2004) Increased expression of p62 in expanded polyglutamine-expressing cells and its association with polyglutamine inclusions. *J. Neurochem.* **91,** 57–68
33. Matsumoto, G., Wada, K., Okuno, M., Kurosawa, M., and Nukina, N. (2011) Serine 403 phosphorylation of p62/SQSTM1 regulates selective autophagic clearance of ubiquitinated proteins. *Mol. Cell* **44,** 279–289
34. Doi, H., Adachi, H., Katsuno, M., Minamiyama, M., Matsumoto, S., Kondo, N., Miyazaki, Y., Iida, M., Tohnai, G., Qiang, Q., Tanaka, F., Yanagawa, T., Warabi, E., Ishii, T., and Sobue, G. (2013) p62/SQSTM1 differentially removes the toxic mutant androgen receptor via autophagy and inclusion formation in a spinal and bulbar muscular atrophy mouse model. *J. Neurosci.* **33,** 7710–7727
35. Schaffar, G., Breuer, P., Boteva, R., Behrends, C., Tzvetkov, N., Strippel, N., Sakahira, H., Siegers, K., Hayer-Hartl, M., and Hartl, F. U. (2004) Cellular toxicity of polyglutamine expansion proteins: mechanism of transcription factor deactivation. *Mol. Cell* **15,** 95–105
36. Kayed, R., Head, E., Thompson, J. L., McIntire, T. M., Milton, S. C., Cotman, C. W., and Glabe, C. G. (2003) Common structure of soluble amyloid oligomers implies common mechanism of pathogenesis. *Science* **300,** 486–489
37. Ravikumar, B., Vacher, C., Berger, Z., Davies, J. E., Luo, S., Oroz, L. G., Scaravilli, F., Easton, D. F., Duden, R., O'Kane, C. J., and Rubinsztein, D. C. (2004) Inhibition of mTOR induces autophagy and reduces toxicity of polyglutamine expansions in fly and mouse models of Huntington disease. *Nat. Genet.* **36,** 585–595
38. Martin, D. D., Ladha, S., Ehrnhoefer, D. E., and Hayden, M. R. (2014) Autophagy in Huntington disease and huntingtin in autophagy. *Trends Neurosci.* 10.1016/j.tins.2014.09.003
39. Brady, O. A., Meng, P., Zheng, Y., Mao, Y., and Hu, F. (2011) Regulation of TDP-43 aggregation by phosphorylation and p62/SQSTM1. *J. Neurochem.* **116,** 248–259
40. Scotter, E. L., Vance, C., Nishimura, A. L., Lee, Y. B., Chen, H. J., Urwin, H., Sardone, V., Mitchell, J. C., Rogelj, B., Rubinsztein, D. C., and Shaw, C. E. (2014) Differential roles of the ubiquitin proteasome system and autophagy in the clearance of soluble and aggregated TDP-43 species. *J. Cell Sci.* **127,** 1263–1278
41. Petrucelli, L., Dickson, D., Kehoe, K., Taylor, J., Snyder, H., Grover, A., De Lucia, M., McGowan, E., Lewis, J., Prihar, G., Kim, J., Dillmann, W. H., Browne, S. E., Hall, A., Voellmy, R., Tsuboi, Y., Dawson, T. M., Wolozin, B., Hardy, J., and Hutton, M. (2004) CHIP and Hsp70 regulate tau ubiquitination, degradation and aggregation. *Hum. Mol. Genet.* **13,** 703–714
42. Shimura, H., Schwartz, D., Gygi, S. P., and Kosik, K. S. (2004) CHIP-Hsc70 complex ubiquitinates phosphorylated Tau and enhances cell survival. *J. Biol. Chem.* **279,** 4869–4876
43. Lee, M. J., Lee, J. H., and Rubinsztein, D. C. (2013) Tau degradation: the ubiquitin-proteasome system versus the autophagy-lysosome system. *Prog. Neurobiol.* **105,** 49–59
44. Iwata, N., Tsubuki, S., Takaki, Y., Watanabe, K., Sekiguchi, M., Hosoki, E., Kawashima-Morishima, M., Lee, H. J., Hama, E., Sekine-Aizawa, Y., and Saido, T. C. (2000) Identification of the major Aβ_{1-42}-degrading catabolic pathway in brain parenchyma: suppression leads to biochemical and pathological deposition. *Nat. Med.* **6,** 143–150
45. Qiu, W. Q., Walsh, D. M., Ye, Z., Vekrellis, K., Zhang, J., Podlisny, M. B., Rosner, M. R., Safavi, A., Hersh, L. B., and Selkoe, D. J. (1998) Insulin-degrading enzyme regulates extracellular levels of amyloid β-protein by degradation. *J. Biol. Chem.* **273,** 32730–32738

Molecular Bases of Disease:

p62 Plays a Protective Role in the Autophagic Degradation of Polyglutamine Protein Oligomers in Polyglutamine Disease Model Flies

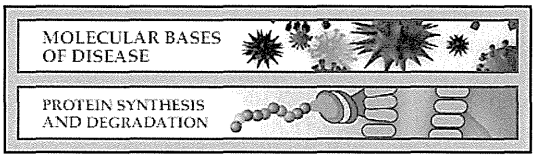

Yuji Saitoh, Nobuhiro Fujikake, Yuma Okamoto, H. Akiko Popiel, Yusuke Hatanaka, Morio Ueyama, Mari Suzuki, Sébastien Gaumer, Miho Murata, Keiji Wada and Yoshitaka Nagai

J. Biol. Chem. 2015, 290:1442-1453.
doi: 10.1074/jbc.M114.590281 originally published online December 5, 2014

Send Orders for Reprints to reprints@benthamscience.net

Current Medicinal Chemistry, 2014, *21*, ????-????

Peptide-Based Therapeutic Approaches for Treatment of the Polyglutamine Diseases

Toshihide Takeuchi[1,3,*], H. Akiko Popiel[1], Shiroh Futaki[3], Keiji Wada[1], and Yoshitaka Nagai[1,2,*]

[1]*Department of Degenerative Neurological Diseases, National Institute of Neuroscience, National Center of Neurology and Psychiatry, Kodaira, Tokyo 187-8502, Japan;* [2]*Core Research for Evolutional Science and Technology (CREST), Japan Science and Technology Agency, Kawaguchi, Saitama 332-0012, Japan;* [3]*Institute for Chemical Research, Kyoto University, Uji, Kyoto 611-0011, Japan*

Abstract: The polyglutamine (polyQ) diseases including Huntington's disease and spinocerebellar ataxias are a group of inherited neurodegenerative diseases that are caused by an abnormal expansion of the polyQ stretch in disease-causative proteins. The expanded polyQ stretches are intrinsically unstable and are prone to form insoluble aggregates and inclusion bodies. Recent studies have revealed that the expanded polyQ proteins gain cytotoxicity during the aggregation process, which may possibly cause detrimental effects on a wide range of essential cellular functions leading to eventual neuronal degeneration. Based on the pathogenic mechanism of the polyQ diseases, several therapeutic approaches have been proposed to date. Among them, here we focus on peptide-based approaches that target either aggregate formation of the polyQ proteins or abnormal cellular processes induced by the expanded polyQ proteins. Although both approaches are effective in suppressing cytotoxicity of the abnormal polyQ proteins and the disease phenotypes of animal models, the former approach is more attractive since it targets the most upstream change occurring in the polyQ diseases, and is therefore expected to be effective against various downstream functional abnormalities in a broad range of polyQ diseases. One of the major current problems that must be overcome for development of peptide-based therapies of the polyQ diseases is the issue of brain delivery, which is also discussed in this article. We hope that in the near future effective therapies are developed, and bring hope to many patients suffering from the currently untreatable polyQ diseases.

Keywords: Neurodegeneration, peptide, polyglutamine diseases, protein aggregation, therapy.

THE POLYGLUTAMINE DISEASES

The polyglutamine (polyQ) diseases are a group of inherited neurodegenerative disorders characterized by a common genetic mutation in the coding sequence of each disease-causative gene, in which a trinucleotide CAG repeat encoding a polyQ stretch is abnormally expanded (>35-40 repeats) [1-3]. So far, nine disorders have been recognized as such diseases, including Huntington's disease (HD), spinal and bulbar muscular atrophy (SBMA), several types of spinocerebeller ataxias (SCAs) [2]. These diseases are all characterized by the progressive degeneration and loss of neurons in various regions of the brain, resulting in progressive neurological and psychiatric symptoms such as cognitive impairment and motor disturbance. No effective treatment for the polyQ diseases has been established to date.

The molecular basis of the polyQ diseases is the abnormal expansion of a polyQ stretch in each host protein. In most cases, the threshold polyQ length for disease manifestation is around 35-40 repeats, as polyQ expansions longer than 40 repeats typically result in the polyQ diseases [3]. For example, the polyQ length in huntingtin (Htt), the causative protein of HD, ranges in size from 5 to 35 repeats in normal subjects, but is expanded to more than 40 repeats in patients with HD [4]. The polyQ length in the disease-causative protein can also affect the disease progression, as it correlates tightly with the age at onset and severity of disease [5, 6]. Animal studies have demonstrated that typical disease phenotypes such as progressive degeneration and loss of neurons in the brain can be caused by expression of the expanded polyQ stretch alone, further supporting the pathological importance of the abnormal expansion of the polyQ stretch [7-11]. These facts strongly indicate that the polyQ diseases are caused by a gain of toxic function mechanism of the expanded polyQ stretch, and are considered to be unrelated with the specific functions of each host protein.

The expanded polyQ stretches are intrinsically unstable, and are likely to form insoluble aggregates and inclusion bodies, which are a common pathological characteristic observed in the brain of polyQ disease patients as well as animal models [12, 13]. The mechanisms as to how expanded polyQ proteins form aggregates and the relationship between aggregate formation and cytotoxicity have been extensively studied [14-18]. Recent accumulating evidence strongly indicate that abnormal intermediate species such as oligomeric intermediates and even misfolded monomers of the expanded polyQ proteins which form prior to aggregates/inclusion bodies could be more toxic to neurons compared with in-

*Address correspondence to this author at the Department of Degenerative Neurological Diseases, National Institute of Neuroscience, National Center of Neurology and Psychiatry, 4-1-1 Ogawa-Higashi, Kodaira, Tokyo 187-8502, Japan; Tels: +81-42-346-1715 and +81-774-38-3211;
Faxes: +81-42-346-1745 and +81-774-32-3038;
E-mails: nagai@ncnp.go.jp and takeuchi@scl.kyoto-u.ac.jp

0929-8673/14 $58.00+.00